Downloaded from orbit.dtu.dk on: Apr 20, 2024

DTU Library

Probing efficient microbial CO_2 utilisation through metabolic and process modelling

Gorter de Vries, Philip J.; Mol, Viviënne; Sonnenschein, Nikolaus; Jensen, Torbjørn Ølshøj; Nielsen, Alex Toftgaard

Published in:
Microbial Biotechnology

Link to article, DOI:
10.1111/1751-7915.14414

Publication date:
2024

Document Version
Publisher's PDF, also known as Version of record

Link back to DTU Orbit

Citation (APA):
Gorter de Vries, P. J., Mol, V., Sonnenschein, N., Jensen, T. Ø., & Nielsen, A. T. (2024). Probing efficient microbial CO_2 utilisation through metabolic and process modelling. *Microbial Biotechnology*, *17*(2), Article e14414. https://doi.org/10.1111/1751-7915.14414

General rights
Copyright and moral rights for the publications made accessible in the public portal are retained by the authors and/or other copyright owners and it is a condition of accessing publications that users recognise and abide by the legal requirements associated with these rights.

- Users may download and print one copy of any publication from the public portal for the purpose of private study or research.
- You may not further distribute the material or use it for any profit-making activity or commercial gain
- You may freely distribute the URL identifying the publication in the public portal

If you believe that this document breaches copyright please contact us providing details, and we will remove access to the work immediately and investigate your claim.

Check for updates

Received: 24 July 2023 | Accepted: 10 January 2024

DOI: 10.1111/1751-7915.14414

MICROBIAL BIOTECHNOLOGY Applied Microbiology International

RESEARCH ARTICLE

Probing efficient microbial CO_2 utilisation through metabolic and process modelling

Philip J. Gorter de Vries[1] | **Viviënne Mol**[1] | **Nikolaus Sonnenschein**[2] | **Torbjørn Ølshøj Jensen**[1,3] | **Alex Toftgaard Nielsen**[1]

[1]The Novo Nordisk Foundation Center for Biosustainability, Technical University of Denmark, Kongens Lyngby, Denmark

[2]Department of Biotechnology and Biomedicine, Technical University of Denmark, Kongens Lyngby, Denmark

[3]Again, Søborg, Denmark

Correspondence
Alex Toftgaard Nielsen, The Novo Nordisk Foundation Center for Biosustainability, Technical University of Denmark, 2800 Kongens Lyngby, Denmark.
Email: atn@biosustain.dtu.dk

Funding information
Villum Fonden, Grant/Award Number: 40986; Horizon 2020 Framework Programme, Grant/Award Number: 101037009; Novo Nordisk Fonden, Grant/Award Number: NNF17SA0031362, NNF18CC0033664, NNF19CC0035454 and NNF20CC0035580; Danmarks Frie Forskningsfond, Grant/Award Number: 103200448B

Abstract

Acetogenic gas fermentation is increasingly studied as a promising technology to upcycle carbon-rich waste gasses. Currently the product range is limited, and production yields, rates and titres for a number of interesting products do not allow for economically viable processes. By pairing process modelling and host-agnostic metabolic modelling, we compare fermentation conditions and various products to optimise the processes. The models were then used in a simulation of an industrial-scale bubble column reactor. We find that increased temperatures favour gas transfer rates, particularly for the valuable and limiting H_2, while furthermore predicting an optimal feed composition of 9:1 mol H_2 to mol CO_2. Metabolically, the increased non-growth associated maintenance requirements of thermophiles favours the formation of catabolic products. To assess the expansion of the product portfolio beyond acetate, both a product volatility analysis and a metabolic pathway model were implemented. In-situ recovery of volatile products is shown to be within range for acetone but challenging due to the extensive evaporation of water, while the direct production of more valuable compounds by acetogens is metabolically unfavourable compared to acetate and ethanol. We discuss alternative approaches to overcome these challenges to utilise acetogenic CO_2 fixation to produce a wider range of carbon negative chemicals.

INTRODUCTION

To meet ambitious climate goals set by governments and institutions across the globe, the current reduction of emitted greenhouse gases (GHG) is not deemed sufficient (Masson-Delmotte et al., 2021). As a result, carbon capture technologies have gained interest and are increasingly being implemented. However, the predominant carbon capture technologies rely on costly storage of sequestered carbon dioxide (CO_2), in large underground reservoirs, where it remains unused (Lackner, 2003). To allow circular re-use of carbon, released or sequestered CO_2 can be upgraded into more valuable biochemicals using Carbon Capture and Utilisation (CCU). CO_2 is a thermodynamically stable form of carbon, and as such, relies on energy input to be condensed into longer carbon chains, for example in CO_2 electroreduction to acetate (Zheng et al., 2022) or ethanol (Jouny et al., 2018). Naturally, microbial cells function as biological catalysts capable of performing chemical reactions with lower energy inputs through their reliance on enzymes. Photosynthesis, the most abundant biologic carbon fixation pathway, harnesses light to reduce CO_2, an energy source that is however poorly scalable in industrial-scale CCU (Chen et al., 2010). Although less abundant, various

Philip J. Gorter de Vries and Viviënne Mol contributed equally and should be considered joint first authors.

This is an open access article under the terms of the Creative Commons Attribution-NonCommercial License, which permits use, distribution and reproduction in any medium, provided the original work is properly cited and is not used for commercial purposes.
© 2024 The Authors. *Microbial Biotechnology* published by Applied Microbiology International and John Wiley & Sons Ltd.

chemoautotrophic ways of life exist, which use chemicals as energy sources. Organisms harbouring such metabolism are more suitable for industrial-scale CCU and can be used to utilise carbon from gasified biomass or industrial waste gas, for example, from the steel industry (Köpke et al., 2011). A main group of interest is organisms using the Wood-Ljungdahl pathway (WLP) to reduce CO_2 or carbon monoxide (CO) to form acetyl-CoA, with redox potential from the oxidation of CO or hydrogen (H_2) (Ragsdale & Pierce, 2008; Wieringa, 1936; Wood & Harris, 1951). The generated acetyl-CoA can be further fermented into various products, including acetate or ethanol (Daniell et al., 2012). The class of bacteria that possess the WLP are acetogens, a polyphyletic group characterised by their main metabolic product: acetate.

The synthetic biology era has facilitated the introduction of novel phenotypes to various microbial hosts. Recent efforts have engineered synthetic microbial cell factories to introduce CO_2 as a carbon source into model organisms such as *Escherichia coli* and *Pichia pastoris*, however, the rates that can be achieved are by far outcompeted by the natural WLP harbouring organisms (Bar-Even et al., 2010; Gassler et al., 2020; Li et al., 2017; Scheffen et al., 2021). To harness the natural efficient CO_2 fixating capabilities, various acetogens have been engineered to produce a wider range of valuable bioproducts (Cheng et al., 2019; Jia et al., 2021; Liew et al., 2017). Recently, the carbon-negative production of acetone and isopropanol by an engineered mesophilic *Clostridium* has been demonstrated up to pilot scale (Liew et al., 2022). Acetogens are a diverse group showing large phenotypic variation, including their optimal growth temperature where mesophilic organisms grow in ranges up to 45°C, and thermophilic hosts have optimum growth temperatures above this threshold. The diversity of commonly used acetogens has been reviewed in regards to their growth temperature optima, ranging from 20 to 66°C, but also other characteristics such as their prevalent metabolic substrates and products (Lee et al., 2022). To date, most engineered acetogens are mesophilic, where only a few examples of engineered thermophilic acetogens producing alternative biochemicals exist (Kato et al., 2021). Temperature is a factor that directly affects virtually all physicochemical aspects of a fermentation process, including the biology. Working under thermophilic conditions provide various advantages over mesophilic production conditions, including decreased contamination risks, lower cooling costs, higher mass transfer rates, a key factor considering the gaseous substrates (Liew et al., 2016), and improved growth and production rates (Krüger et al., 2018; Zeldes et al., 2015). Additionally, higher fermentation temperatures allow more efficient in situ product recovery through gas stripping, specifically for volatile products. This facilitates simple downstream processing, whilst keeping product buildup in the fermentation broth low, in turn preventing product toxicity and feedback inhibition of production pathways (Brennan et al., 2012; Verhoef et al., 2009). As a result of these advantages, previously the economic feasibility of producing a volatile organic compound (VOC), acetone, from a theoretical thermophilic production strain was shown (Redl, Diender, et al., 2017). In the present study, we investigate the effect of process temperature on industrial acetogenic CO_2 fixation by using biological and mass transfer models, focusing especially on the effects of temperature on metabolism, gas uptake rates and gas stripping effectivity. These models are used as inputs for a bioprocess design and included in a final computational simulation of the chosen production process, as illustrated in Figure 1, thereby highlighting the importance of tailoring biological parameters to process and product requirements.

In bioprocess engineering, the choice of the host organism is often the first decision to be made. However, this choice is often limited to a few model organisms, or even more restrictive, to the specific organism that researchers have predominant experience with. While engineering might increase the performance of the specific organism under the desired conditions, better characteristics may be achievable by choosing a starting organism that is innately more suited to the envisioned product and hence required process. To capture this ambiguous starting point, and let process requirements dictate ensuing host selection, a host-agnostic bacterial model of microbial growth dynamics can be used, based only on universal overall reaction stoichiometry and general microbial growth properties (Pirt, 1965).

As summarised in Figure 1, we start with assessing the substrate solubilisation by modelling the gas–liquid mass transfer rates through two-film mass transfer theory. We then investigate the effect of temperature on acetogenic growth using temperature dependent, host-agnostic black box biological models of acetogenic yields. These two models are then used in a process simulation for acetate production in an industrial-scale Bubble Column Reactor (BCR). To test the possibility of expanding the product portfolio beyond acetate, we model acetogenic metabolism in more detail using a stoichiometric model of the WLP, thereby comparing the energetic balance of different possible products. A comparison of vapour pressures for a range of VOCs tests the feasibility of in-situ product recovery.

EXPERIMENTAL PROCEDURES

In the presented work, we combine thermodynamics-based reactor modelling, building upon the findings of Redl, Sukumara, et al. (2017), with steady-state stoichiometric modelling of metabolism. All calculations and simulations were done in Jupyter Notebooks, freely

17517915, 2024, 2, Downloaded from https://ami-journals.onlinelibrary.wiley.com/doi/10.1111/1751-7915.14414 by Danish Technical Knowledge, Wiley Online Library on [23/02/2024]. See the Terms and Conditions (https://onlinelibrary.wiley.com/terms-and-conditions) on Wiley Online Library for rules of use; OA articles are governed by the applicable Creative Commons License

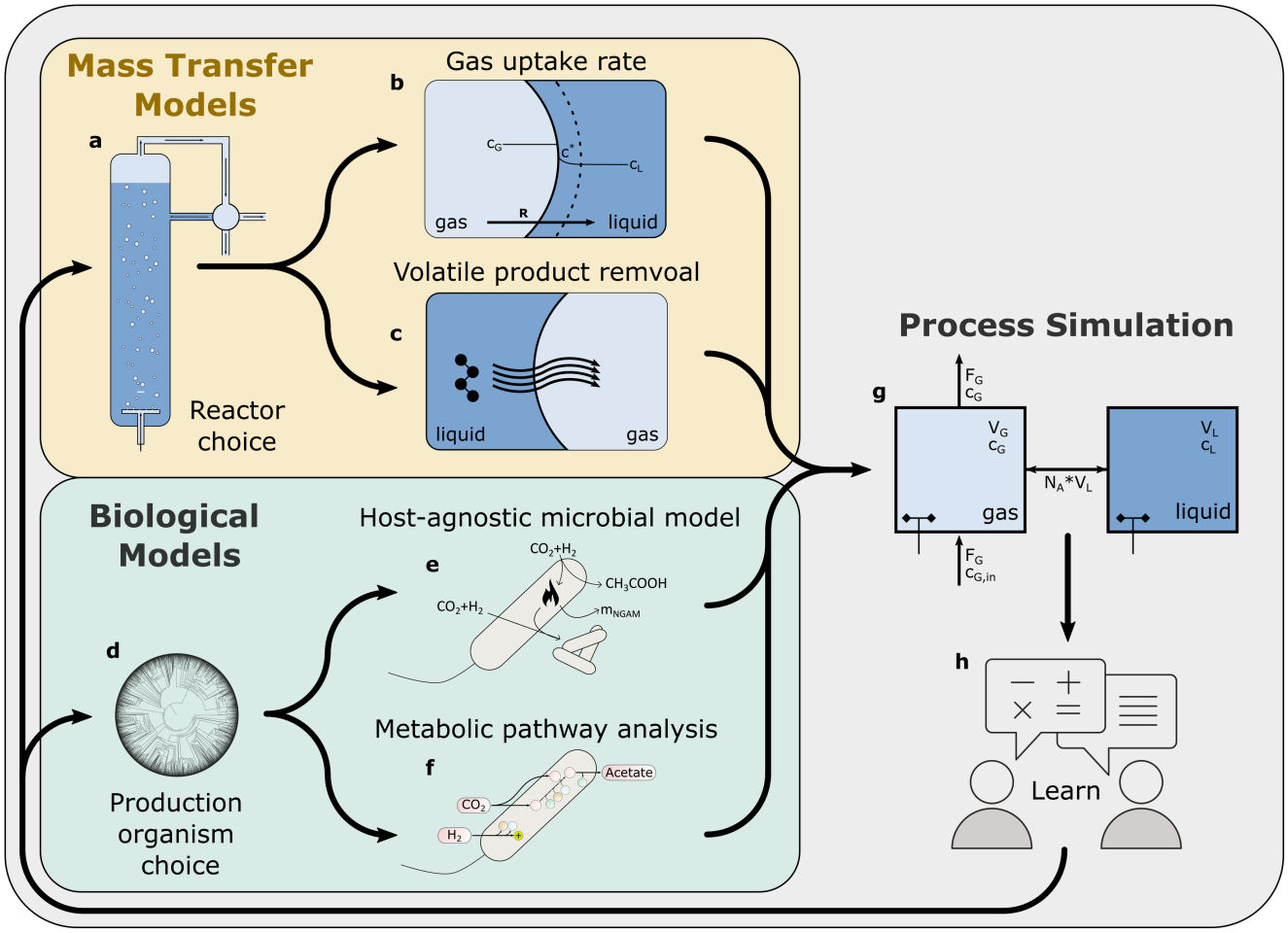

FIGURE 1 Overview of the models used in this work. Starting with a choice of reactor (A), mass transfer for both the gas substrate uptake rates (B) and the volatile product recovery are modelled (C). For a chosen production organism (D), a model based on general microbial growth, overall stoichiometry and reaction thermodynamics is built (E), complemented with a more detailed stoichiometric pathway analysis (F). These models are used to run a process simulation (G) of which the learnings (H) are used to reevaluate the initial choices.

available on GitHub (https://github.com/biosustain/CO2_fixation_models/releases/tag/v3.0), using python 3.8, extended with the Numpy (Harris et al., 2020), SciPy (Virtanen et al., 2020) and Pandas (Mckinney, 2010) packages, and Matplotlib (Hunter, 2007) for plotting. Additional packages used are listed in specific sections below. Illustrations are made with the open-source vector image software Inkscape.

Reactor properties

The reactor setup used in the simulations is a 30-m-tall BCR with a radius of 3 m, filled to 2/3 of its volume (Redl, Sukumara, et al., 2017). It is continuously fed with a mix of H_2 and CO_2. The feed rate is adjusted to obtain a superficial gas velocity (v_{gs}^c) (Clark & Blanch, 1995) of 0.1 m/s, in the range of conventional values for large scale BCRs (Redl, Sukumara, et al., 2017; van Baten & Krishna, 2004). The reactor is modelled as two ideally mixed entities, the gas phase, which represents all gas bubbles passing through the column, and the broth. Only the gas phase has a continuous flow-through. Exchanges between both phases are modelled as a single transfer rate for each compound. Unless specified otherwise, the temperature range used in the various aspects modelled is between 0 and 80°C, corresponding to 273.15–353.15 K. Further parameters, including the liquid volume (V_L), the gas holdup fraction (ε) (Heijnen & Van't Riet, 1984), the pressure at the bottom of the tank (P_b) and the logarithmic mean pressure (P_m) (Clark & Blanch, 1995) were defined from the basic properties of the reactor (Equations 1–5). Constants and physio-chemical values are named in the nomenclature and their values are listed with their sources in Tables S3, S4 and S5.

Superficial gas velocity:

$$v_{gs}^c = F_a v / \left(\pi * r^2\right) / 3600 \left[\mathrm{m/s}\right] \quad (1)$$

Liquid volume, assuming 2/3 filled:

$$V_L = \pi * r^2 * h * 2/3 \left[\mathrm{m}^3\right] \quad (2)$$

17517915, 2024, 2, Downloaded from https://ami-journals.onlinelibrary.wiley.com/doi/10.1111/1751-7915.14414 by Danish Technical Knowledge, Wiley Online Library on [23/02/2024]. See the Terms and Conditions (https://onlinelibrary.wiley.com/terms-and-conditions) on Wiley Online Library for rules of use; OA articles are governed by the applicable Creative Commons License

Gas holdup fraction:

$$\varepsilon = 0.6 * \left(v_{gs}^{c}\right)^{0.7} \quad (3)$$

Pressure at the bottom, assuming 2/3 filled:

$$P_b = P_t + h * 2/3 * 1000 * g \ [\mathrm{Pa}] \quad (4)$$

Logarithmic mean pressure:

$$P_m = \left(P_b - P_t\right) / \log\left(P_b / P_t\right) \ [\mathrm{Pa}] \quad (5)$$

Gas–liquid mass transfer

To address the inflow and outflow terms of the mass balance, the mass transfer rates were determined for each compound across the gas–liquid phase boundary using the two-film theory (Doran, 2013; Whitman, 1962). In two-film theory, the division between two phases is seen as a boundary where each phase forms a film providing resistance to the mass transfer. The mass transfer through each of the boundary films (R) was expressed for each compound as a function of a coefficient (k), the surface area of the interface (a) and the concentration difference between the bulk of the phase and the interface. For gases that are poorly soluble in water, the liquid-side film resistance was assumed to be dominant and the gas-side resistance negligible. This was done for CO_2, CO, H_2, O_2 and N_2 (notebook 01). The factors k and a were combined into a single term: $k_L a$. The transfer rate is therefore a function of the volumetric mass transfer coefficient $k_L a$, the saturation concentration and the dissolved concentration in the liquid (Equation 6). The value of $k_L a$ is specific to both the reactor and the compound. For a coarse bubble system in the dimension range of the envisioned BCR, $k_L a$ of O_2 at 20°C was expressed as a function of the superficial gas velocity (Heijnen & Van't Riet, 1984). The $k_L a$ of all other compounds was extrapolated from that O_2 using the diffusion coefficient of the new compound and the reference (Munz & Roberts, 1989; Equation 7). Furthermore, $k_L a$ was expressed as a function of temperature by multiplying by the correction factor θ, to the power of the temperature difference (Equation 8; Heijnen & Van't Riet, 1984).

The concentrations of dissolved gases at the liquid side of the interface were assumed to be at equilibrium, thus equal to the saturation concentration of the gas in water. This saturation concentration (c^*) was expressed according to Henry's law, as a function of a compound- and temperature-dependent constant (H_T), the mol fraction in thegas and the pressure (p), for which the mean logarithmic pressure is used (Sander, 2023; Equation 9). H_T was expressed as temperature-dependent expression, containing a known value of H at a given reference temperature, a compound-specific temperature correction factor k_h based on the van 't Hoff equation, and the reference temperature (Sander, 2023; Equation 10).

Transfer rate:

$$R_i = k_L a_T * \left(c^* - c_l\right) \left[\mathrm{mol}/\mathrm{m}^3/\mathrm{s}\right] \quad (6)$$

Volumetric mass transfer coefficient:

$$k_L a_{20} = 0.32 * \left(D_i / D_{O_2}\right)^{0.5} * \left(v_{gs}^{c}\right)^{0.7} \ [1/\mathrm{s}] \quad (7)$$

Temperature corrected volumetric mass transfer coefficient:

$$k_L a_T = k_L a_{20} * \theta^{T-293.15} [1/\mathrm{s}] \quad (8)$$

Saturation concentration:

$$c^* = H_T * y * P \left[\mathrm{mol}/\mathrm{m}^3\right] \quad (9)$$

Temperature-corrected Henry's law constant:

$$H_T = H_0 * e^{\left[k_H * ((1/T) - (1/298.15))\right]} \left[\mathrm{mol}/\mathrm{m}^3 * \mathrm{Pa}\right] \quad (10)$$

Acetogen thermodynamic black box model

Acetogenic yields were deduced from the overall reaction stoichiometries. These are established by determining the substrates and products and balancing the obtained equations (Shuler & Kargi, 2002). Two reactions were defined, the catabolic reaction producing acetic acid (Equation 11) and the anabolic reaction producing biomass (Equation 12). The biomass composition was assumed to be $CH_{1.8}O_{0.5}N_{0.2}$ (Heijnen, 2010). To meet the nitrogen requirements of the anabolic reactions, ammonia (NH_3) was included as a substrate.

Catabolic reaction stoichiometries:

$$2CO_2 + 4H_2 \Longleftrightarrow CH_3COOH + 2H_2O \quad (11)$$

Anabolic reactions stoichiometries:

$$CO_2 + 2.1H_2 + 0.2NH_3 \Longleftrightarrow CH_{1.8}O_{0.5}N_{0.2} + 1.5H_2O \quad (12)$$

With the anabolic and catabolic reactions determined, the energy generated by catabolism and energy needed for anabolism were determined. Firstly, to determine the energy generated by catabolism, the Gibbs free energy of reaction (ΔG_r) was calculated as a temperature-dependent function based on the Gibbs–Helmholtz equation (Equation 15). This equation corrects the Gibbs free energy of reaction by temperature, based on the Gibbs free energies of reaction and reaction enthalpy at standard conditions (ΔG_f^0 & ΔH_f^0), both being the difference of the Gibbs free energies and enthalpies of the products and substrates (Equations 13 and 14, Table S6). Secondly, the anabolic energy

17517915, 2024, 2, Downloaded from https://ami-journals.onlinelibrary.wiley.com/doi/10.1111/1751-7915.14414 by Danish Technical Knowledge, Wiley Online Library on [23/02/2024]. See the Terms and Conditions (https://onlinelibrary.wiley.com/terms-and-conditions) on Wiley Online Library for rules of use; OA articles are governed by the applicable Creative Commons License

requirement corresponding to the GAM was calculated. For autotrophic growth, GAM depends primarily on the nature of the electron donor (Heijnen, 2010). It was thus estimated by extrapolation from other organisms to be 1000 kJ/$Cmol_{biomass}$ (Heijnen, 2010). The overall reaction stoichiometries were predicted for any given temperature by finding the factor by which to multiply the catabolic reaction so that it generates the 1000 kJ that is required for the growth of 1 $Cmol_{biomass}$ (Equation 16). These stoichiometries were then used to determine the yields of product on substrate (Y_{PS}), biomass on substrate (Y_{XS}), etc. by dividing the respective stoichiometric factors as ratios. NGAM is not included in the yields, as it is dependent on the specific growth rate. It is accounted for later, in the black box model.

Gibbs free energy of reaction:

$$\Delta_r G^0 = \sum_i v_i * \Delta_f G_i^0 \ \left[\mathrm{kJ/mol}\right] \tag{13}$$

Reaction enthalpy:

$$\Delta_r H^0 = \sum_i v_i * \Delta_f H_i^0 \ \left[\mathrm{kJ/mol}\right] \tag{14}$$

Gibbs–Helmholtz equation:

$$\Delta_r G^T = \Delta_r G^0 * (T/298.15) + \Delta_r H^0 * (1 - T/298.15) \ \left[\mathrm{kJ/mol}\right] \tag{15}$$

$$S_I = S_{I,\mathrm{ana}} + \frac{m_{\mathrm{GAM}}(T) * S_{X,\mathrm{ana}}}{-\Delta_r G(T) * S_{P,\mathrm{cata}}} * S_{\mathrm{I,cata}} \tag{16}$$

Building on the calculations above, a black box model was created for hydrogenotrophic growth. The model used here consists only of growth, consumption and production rates, assuming a single rate-limiting substrate, namely the electron donor, H_2. The specific growth rate is modelled using the Monod equation (Monod, 1949), with a product inhibition term (Equation 18; Levenspiel, 1980). Values for the saturation constant (K_S) and the inhibitory product concentration (c_P^*) were obtained from literature or estimated (Table S7). The maximum growth rate of acetogens (μ_{max}) was predicted as a function of temperature with the Arrhenius equation (Equation 17), a model inspired by reaction kinetics, used in ecology and food safety (De Silvestri et al., 2018; Huang et al., 2011; Ingraham, 1958; Price & Sowers, 2004; Servais et al., 1985). The equation is a function of temperature containing three parameters: the gas constant (R), an equation-specific constant (A) and a substitute for the activation energy (B). To determine these parameter values, the function was fit to the maximum growth rates of 34 known acetogens found in literature, plotted by their optimum growth temperature. These values are listed in Table S8 and were fitted using SciPy (Figure S1C), which set the parameters to be $A = 8.66$ and $B = 24166.93$.

The Arrhenius equation for max growth rate:

$$\mu_{\max} = A * T * e^{-B/(R*T)} \ \left[h^{-1}\right] \tag{17}$$

Specific substrate consumption rates follow Pirt kinetics and the same applies for product formation, as long as the product is formed in the catabolic reaction (Equation 19; Pirt, 1965), with the maintenance term (m_i) defining how much product or substate is formed or consumed through additional catabolic reaction needed to satisfy NGAM energy requirements (Equation 20).

Monod equation, specific growth rate:

$$\mu = \mu_{\max} * \frac{c_S}{K_S + c_S} * \left(1 - c_P / c_P^*\right) \left[\mathrm{h}^{-1}\right] \tag{18}$$

Pirt kinetics, specific consumption and production rate:

$$q_i = \frac{\mu}{Y_{Xi}} + m_{\mathrm{NGAM},i} \left[\mathrm{h}^{-1}\right] \tag{19}$$

$$m_{\mathrm{NGAM},i} = \frac{m_{\mathrm{NGAM}}}{\Delta_r G^T * Y_{PS,\mathrm{cata}}} \left[\mathrm{h}^{-1}\right] \tag{20}$$

Similar to the maximum growth rate, NGAM correlates with temperature. Based on a wide range of studied anaerobic organisms, NGAM can be estimated through the temperature-dependent expression based on the Arrhenius expression, as proposed by Tijhuis et al. (1993) (Equation 21). This equation is compared to a new fit to their data in Figure S1B.

NGAM:

$$m_{\mathrm{NGAM}} = 3.3^{69000/R*(1/298 - 1/T)} \left[\mathrm{KJ/h/Cmol_{biomass}}\right] \tag{21}$$

To assess and compare the energy generated to produce a wider variety of compounds, the catabolic reaction was determined using the same method as for acetate. With the reaction stoichiometry, ΔG_r is the difference of ΔG_f of the products and the substrates for acetate, acetone, ethanol, propanol, butanol and butyrate (Shuler & Kargi, 2002).

Reactor simulation

To simulate the change for each of the modelled compounds over time, a mass balance is set up over the system boundaries, either being the gas phase, liquid phase or both (box 1). This mass balance defines the change in concentration as the sum of inflow, outflow, production and consumption rates (Doran, 2013).

To find the optimal operation setting, the mass balances are solved at steady state, where the accumulation is null. Starting with the mass balance over the substrates in the gas phase and assuming that mass

17517915, 2024, 2, Downloaded from https://ami-journals.onlinelibrary.wiley.com/doi/10.1111/1751-7915.14414 by Danish Technical Knowledge, Wiley Online Library on [23/02/2024]. See the Terms and Conditions (https://onlinelibrary.wiley.com/terms-and-conditions) on Wiley Online Library for rules of use; OA articles are governed by the applicable Creative Commons License

BOX 1 Mass balances; Accumulation = In − Out + Production − Consumption.

Biomass: $\frac{dc_X}{dt} = \mu * c_X$

Acetate: $\frac{dc_{Actt}}{dt} = q_{actt} * c_X$

CO_2, dissolved: $\frac{dc_{CO_2}}{dt} = q_{CO_2} * c_X + R_{CO_2}$

CO, dissolved: $\frac{dc_{CO}}{dt} = q_{CO} * c_X + R_{CO}$

H_2, dissolved: $\frac{dc_{H_2}}{dt} = q_{H_2} * c_X + R_{H_2}$

CO_2, gas: $\frac{dc_{G,\ CO_2}}{dt} = \frac{F_G}{V_G} * \left(c_{G,\ CO_2,in} - c_{G,\ CO_2}\right) - R_{CO_2} * \frac{V_L}{V_G}$

CO, gas: $\frac{dc_{G,CO}}{dt} = \frac{F_G}{V_G} * \left(c_{G,CO,in} - c_{G,\ CO}\right) - R_{CO} * \frac{V_L}{V_G}$

H_2, gas: $\frac{dc_{G,\ H_2}}{dt} = \frac{F_G}{V_G} * \left(c_{G,\ H_2,in} - c_{G,\ H_2}\right) - R_{H_2} * \frac{V_L}{V_G}$

transfer is limiting, thus that its dissolved concentration is null, the gas concentration at steady state can be expressed as functions of the feed concentration (Box 2). Similarly, one can predict the maximal achievable biomass concentration, which could be reached at steady state. At this biomass concentration, all available substrate is required to satisfy maintenance requirements.

Plotting these results makes it possible to find the tipping point where the limiting substrate changes, namely the intersection of the defined functions for CO_2 and H_2. These points change with temperature as described in the results section. The gas feed composition at these tipping points was used as a parameter for further simulations. To simulate the reactor run at 30 and 60°C, the set of differential equations (Box 1) was integrated using SciPy, with given initial conditions, and defined functions for growth (μ), production and consumption rates (q) and mass transfer rates (R).

Volatile product recovery

To model the transfer of compounds from the liquid to the gas phase, namely evaporation of possible volatile products, the boiling points and diffusion rates were expressed for each compound as functions of temperature. The vapour pressure is key for calculating both, it determines the saturation concentration in the gas for modelling diffusion using two-film theory and sets the boiling point as the temperature where the vapour pressure exceeds ambient pressure. In this analysis, acetate, methanol, ethanol, propanol, butanol, butanone, acetone, butyrate and butanediol were included and water was used as a reference. Vapour pressure is temperature dependent and was thus defined for any compound as a function of temperature, using either the Antoine equation (Rumble et al., 1994; Equations 22 and 23) or the Clausius-Clapeyron equation (Carnot, 1824; Equation 24), or an approximation thereof (Rumble et al., 1994; Equations 25 and 26). The gas was assumed to be ideally mixed and fully saturated by the time it leaves the column.

Antoine equation:

$$\log_{10}\left(P_T / P_0\right) = A_1 - A_2 / \left(T + A_3\right) \quad (22)$$

$$P(T) = 10^{A_1 - A_2/(T+A_3)} * P_0 \quad (23)$$

Clausius-Clapeyron equation:

$$P(T) = e^{\Delta_{vap}H/RT + C} \quad (24)$$

Clausius-Clapeyron approximation:

$$\Delta T / \Delta P = RT_b^2 / \left(P_0 * \Delta_{vap}H\right) \quad (25)$$

$$P(T) = RT_b^2 / \left(P_0 * \Delta_{vap}H\right) * T + C \quad (26)$$

When compared, the Antoine and Clausius-Clapeyron equations yield highly similar curves, while the approximation is only good for temperatures within 10–15°C of boiling point (Figure S2). Therefore, the Clausius-Clapeyron equation was used, which is preferred over the Antoine equation because it requires fewer parameter inputs. Indeed, the pressure can be temperature corrected based only on the molar enthalpy of vaporisation (ΔH_{vap}) and a constant C, which is first fitted from a known vapour pressure at a given reference temperature.

The vapour pressure is also linearly dependent on the concentration of the given compound, the partial vapour pressure follows Raoult's law (Equation 27): the partial vapour pressure (P_i) of each component of an ideal mixture of liquids is equal to the vapour pressure of the pure component (P_i^*) multiplied by its mole fraction in the mixture (x_i).

Raoult's law

$$P_i = P_i^* * x_i \ [\mathrm{Pa}] \quad (27)$$

Because the boiling point is directly determined by the ambient pressure, and this pressure increases in the reactor with the depth in the broth, the pressure was expressed as a function of depth using Pascal's law (Equation 28), assuming a broth density equal to that of water, 1000 kg/m^3, also used to determine the pressure at the bottom of the reactor (Equation 4).

Pascal's law

$$P(h) = \rho * g * h + P_0 \ [\mathrm{Pa}] \quad (28)$$

17517915, 2024, 2, Downloaded from https://ami-journals.onlinelibrary.wiley.com/doi/10.1111/1751-7915.14414 by Danish Technical Knowledge, Wiley Online Library on [23/02/2024]. See the Terms and Conditions (https://onlinelibrary.wiley.com/terms-and-conditions) on Wiley Online Library for rules of use; OA articles are governed by the applicable Creative Commons License

BOX 2 Derivation of steady state equilibria.

Optimal gas feed composition

An equation for $c_{G,i}$ at steady state can be deduced starting with the gas phase mass balance.

$$\frac{dc_{G,i}}{dt} = \frac{F_G}{V_G} * \left(c_{G,i,\text{in}} - c_{G,i}\right) - R_i * \frac{V_L}{V_G} = 0$$

$$c_{G,i} = c_{G,i,in} - R_i * \frac{V_L}{F_G}$$

$$c_{G,i} = c_{G,i,in} - R_i * \frac{h}{v_{gas}}$$

$$c_{G,i} = c_{G,i,\text{in}} - k_L a_{i,T} * \left(c^*_{i,L,T} - c_{i,L}\right) * \frac{h}{v_{gas}}$$

For the limiting substrate *i*, at steady state, where all of it is consumed in the liquid (i.e. $c_{i,L} = 0$), we have:

$$c_{G,i} = c_{G,i,\text{in}} - k_L a_{i,T} * c^*_{i,L,T} * \frac{h}{v_{gas}}$$

$$c_{G,i} = c_{G,i,\text{in}} - k_L a_{i,T} * H_{T,i} * y_i * P * \frac{h}{v_{gas}}$$

Using the ideal gas law, Raoult's law and yields:

$$y_i * P = c_{G,i} * R * T$$

$$c_{G,i} = c_{G,i,\text{in}} - k_L a_{i,T} * H_{T,i} * c_{G,i} * R * T * \frac{h}{v_{gas}}$$

$$c_{G,i} + k_L a_{i,T} * H_{T,i} * c_{G,i} * R * T * \frac{h}{v_{gas}} = c_{G,i,\text{in}}$$

$$c_{G,i} * \left(1 + k_L a_{i,T} * H_{T,i} * R * T * \frac{h}{v_{gas}}\right) = c_{G,i,\text{in}}$$

$$c_{G,i} = \frac{c_{G,i,\text{in}}}{1 + k_L a_{i,T} * H_{T,i} * R * T * \frac{h}{v_{gas}}}$$

Maximum steady-state biomass concentration:

Using the liquid phase mass balance, we predict the maximum achievable biomass concentration, where all substrate is required for maintenance.

Mass balance of compound *i* in the liquid, with $\mu = 0$:

$$q_i = \frac{\mu}{Y_{Xi}} + m_{\text{NGAM},i} = m_{\text{NGAM},i} = \frac{m_{\text{NGAM}}}{-\Delta_r G^T} * S_{i,\text{cata}}$$

$$\frac{dc_i}{dt} = q_i * c_{x,\max} + R_i = 0$$

$$c_{x,\max} = \frac{-R_i}{m_{\text{NGAM},i}}$$

$$c_{x,\max} = \frac{R_i * \Delta_r G^T}{m_{\text{NGAM}} * S_{i,\text{cata}}}$$

17517915, 2024, 2, Downloaded from https://ami-journals.onlinelibrary.wiley.com/doi/10.1111/1751-7915.14414 by Danish Technical Knowledge, Wiley Online Library on [23/02/2024]. See the Terms and Conditions (https://onlinelibrary.wiley.com/terms-and-conditions) on Wiley Online Library for rules of use; OA articles are governed by the applicable Creative Commons License

For the chosen BCR, the steady state product concentration is expressed as a function of temperature (Figure 5C). With H_2 limited growth, ignoring product inhibition, the production rate of the compounds is related to the H_2 uptake rate, calculated earlier, at a 9:1 H_2 to CO_2 ratio, using the stoichiometric yields based overall reaction balancing of CO_2 and H_2 as substrate and the compound of interest and water as products (Table S2). The removal rate divided by the dilution rate gives the concentration in the off-gas, which is converted to a partial pressure using the ideal gas law. From the partial pressure divided by the vapour pressure of the pure compound, a molar fraction can be calculated, assuming that a steady state is reached, which is converted to a concentration.

Stoichiometric model of WL pathway

All stoichiometric modelling was done using COBRApy, a package for constraints-based metabolic modelling for Python (Ebrahim et al., 2013). A stoichiometric model was created of the WLP with all its possible products, taking the iHN637 Genome-scale model of *Clostridium ljungdahlii* DSM 13528 as a template (Nagarajan et al., 2013). For investigation of downstream products of the WLP, a branching pathway to acetone production was created by adding the reactions Acetate-acetoacetate CoA-transferase (ctfAB), and acetoacetate decarboxylase (ADC), involved in acetone production by *Clostridium acetobutylicum* (Matta-El-Amouri et al., 1985). Sink reactions were created for all energy and redox metabolites (ATP/ADP/Pi, NADPH/NADP, NADH/NAD, Ferredoxin o/r, H^+). Flux Balance Analysis (FBA) was used to predict fluxes. The generation and usage of energy and redox intermediates was taken directly from the predicted flux of the sink reactions (notebook 06), determined first upstream of acetyl-CoA, separately for growth on CO and H_2, then downstream for each product. A map was created to visualise the predicted fluxes, using the Escher package (Figure S3). This model was extended to create a second model that includes all relevant bifurcating enzymes. All sinks except ATP/ADP/Pi were removed and four bifurcating enzymes were added: Ferredoxin: NADP reductase, ATP synthase, Ferredoxin NADH linked hydrogenase and Ferredoxin:NAD oxidoreductase. For FBA, the product transportation reaction is set as the objective function and either CO_2 or CO uptake is set to be limiting (notebook 07).

RESULTS

As a starting point of this study, initial process design considerations had to be made. For a bioprocess with gaseous substrate, mass transfer rates tend to be limiting. Reactor types with high gaseous mass transfers are thus suitable. BCRs are conceptually the simplest version of a high transfer rate reactor and are considered to be the benchmark for industrial scale processes reliant on efficient gas transfer (Heijnen & Van't Riet, 1984). They consist of a tall column with pressurised air being injected at the bottom and few moving parts. This simplicity allows for a bioprocess using gaseous substrates with low operation and maintenance costs. Other reactors, such as packed bed reactors (Steger et al., 2022) or U-loops (Puiman et al., 2022) have even higher gas transfer rates (Nikakhtari & Hill, 2005) but are more complex and costly and so were not included in the present work. Based on a thermodynamic and economic assessment of syngas fermentation by Redl et al (Redl, Sukumara, et al., 2017). focused on maximising gas uptake whilst remaining within practical limits, we decided to simulate a 30-m-tall BCR with a radius of 3 m, continuously fed with 10,000 m^3/h of gas.

Gas–liquid mass transfer rates favour thermophilic conditions

While higher temperatures tend to favour mass transfer rates, they decrease gas solubility, making the interplay between the two difficult to predict. To investigate the overall effect of temperature on gas saturation concentrations and diffusion rates, the uptake rates of gaseous substrates into the fermentation broth were modelled. Two-film mass transfer theory (Whitman, 1962) was used to investigate the effects of temperature on the volumetric mass transfer rate (R) through the combined effects of saturation concentration (c^*), volumetric mass transfer coefficient (k_La) and concentration of dissolved gas in the liquid. Both c^* and k_La are temperature dependent and specific to the compound, but k_La is additionally also dependent on the reactor type and operation. Therefore, k_La is modelled for a large-scale BCR type as chosen and described above. For calculation purposes, the broth is assumed to be pure water, meaning that both k_La and c^* are unaffected by media components or products formed, which would be the case in real fermentations. In this analysis, but not the later simulation, full microbial conversion of all dissolved gasses is assumed, meaning that c_L is null. R and its components are expressed as functions of temperature and presented in Figure 2A–D.

While the saturation concentrations of all gasses decrease as temperature increases (Figure 2B), the volumetric mass transfer coefficient, increases exponentially (Figure 2C). Combining these two factors to calculate the overall gas transfer rate shows that the k_La impacts overall transfer rates most in the case of CO, H_2, N_2 and O_2 (Figure 2D). The overall

17517915, 2024, 2, Downloaded from https://ami-journals.onlinelibrary.wiley.com/doi/10.1111/1751-7915.14414 by Danish Technical Knowledge, Wiley Online Library on [23/02/2024]. See the Terms and Conditions (https://onlinelibrary.wiley.com/terms-and-conditions) on Wiley Online Library for rules of use; OA articles are governed by the applicable Creative Commons License

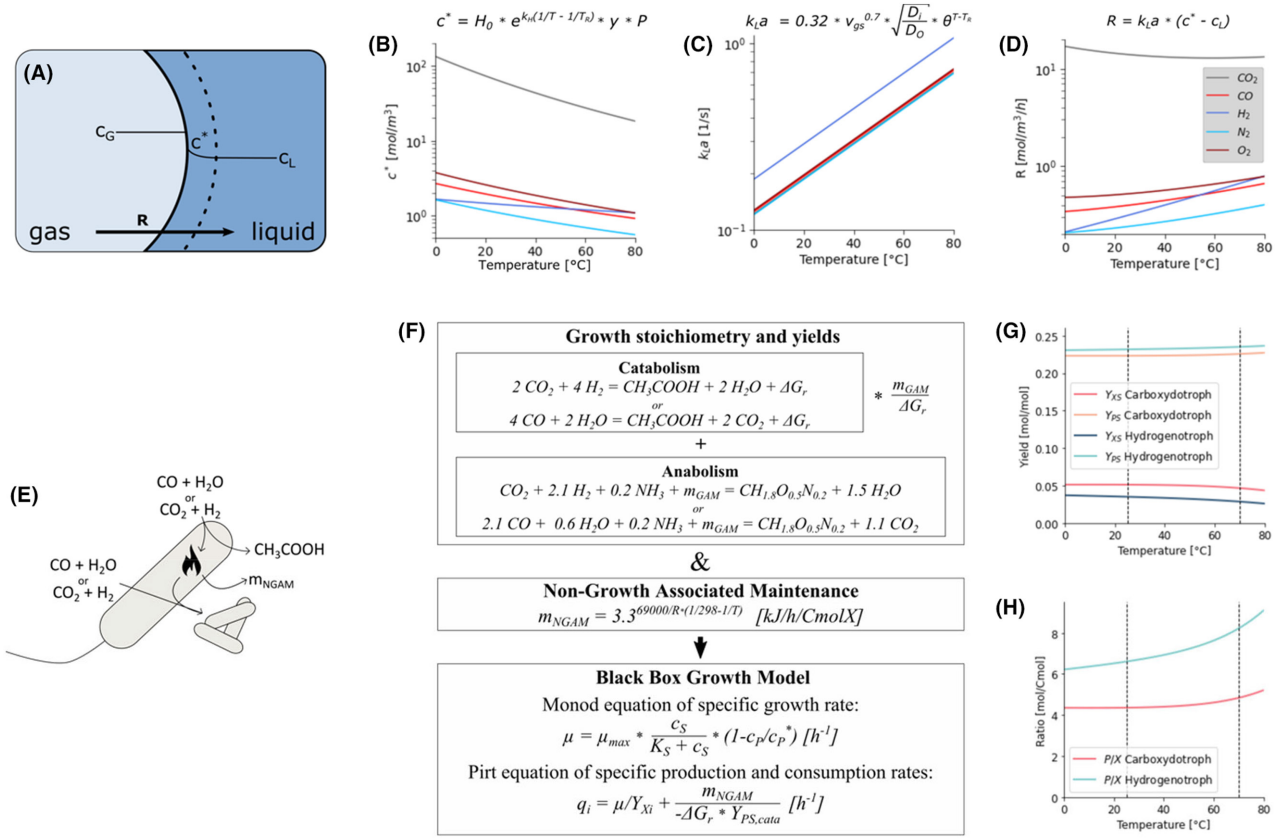

FIGURE 2 Mass transfer modelling of gaseous substrate uptake (A–D) and host agnostic black box microbial model (E–H) for CO_2 fixation to acetate. Temperature-dependent changes in saturation concentrations (B), k_La (C), and the overall volumetric gas transfer rate (D) for CO_2, CO, H_2, N_2 and O_2, assuming gas transfer is limiting. Illustration of the black-box metabolic model (E), how it was built, including reaction thermodynamics, maintenance requirements and maximum growth rate (F), and the resulting comparison of acetogenic growth and production yields on substrate (G) and product to biomass ratio (H) as a function of temperature.

transfer rate of CO_2 decreases, but only by 3% between 30 and 80°C, remaining an order of magnitude higher than the other gasses. O_2 and CO transfer rates increase by around 1.5-fold, while especially the transfer rate of H_2 increases steeply, by 2.4-fold over the same temperature range. For H_2, this is a combination of having the highest k_La and a saturation concentration least affected by temperature. Considering that H_2 is the most expensive and hence often rate limiting gas in acetogenesis, this is an important improvement for overall CO_2 fixation rates of the process. Thus, the volumetric mass transfer rate, and not the gas solubility, dictates the availability of the gaseous substrates, specifically favouring higher temperature operation.

With k_La being inherently dependent on the reactor type, size and operation, these observations cannot be generalised to all setups. If the k_La values differ, their contribution to the volumetric gas transfer rate will change, which should be investigated per reactor type. However, with saturation concentration not being affected by a reactor choice, this effect would thus be even more pronounced for reactor types with higher mass transfer rates.

Temperature dependence of acetogenic yields

Thermodynamic effects are not limited to the physics of gas transfers, but also affect chemical reactions and accordingly, the metabolism of cell factories. Considering the metabolic diversity of acetogens, host agnostic modelling was here applied to capture population complexity, as often performed in microbial ecology or food preservation. To this end, the growth parameters of specific organisms are substituted by the maximum possible growth rate of microbes as a whole. It has been observed that both the growth rate and the death rate of such mixed samples follow the same exponential increase as the Arrhenius equation, used to model the temperature dependence of reaction rates (Davey, 1993; De Silvestri et al., 2018; Ingraham, 1958; Price & Sowers, 2004; Servais et al., 1985). The microbial death rate is conceptually a different way to account for the same biological phenomenon as the Non-Growth Associated Maintenance (NGAM), a parameter to account for yield variation with growth rates (Pirt, 1965). Thus, a temperature-dependent, host agnostic model was

17517915, 2024, 2, Downloaded from https://ami-journals.onlinelibrary.wiley.com/doi/10.1111/1751-7915.14414 by Danish Technical Knowledge, Wiley Online Library on [23/02/2024]. See the Terms and Conditions (https://onlinelibrary.wiley.com/terms-and-conditions) on Wiley Online Library for rules of use; OA articles are governed by the applicable Creative Commons License

made, where the maximum growth rate (μ_{max}), NGAM and the growth and production yields that serve as inputs for Monod and Pirt kinetics (Pirt, 1965). The growth and production yields are deduced from the overall reaction stoichiometries, which in turn is predicted by balancing out the Gibbs free energy of reaction (ΔG_r) generated by catabolism with the Growth-Associated Maintenance (GAM; Figure 2F). As acetate is the main product from gas fermenting acetogens, we focus further efforts on this product, although this can be exchanged for other WLP products of interest.

With increasing temperature, the predicted product to biomass ratio increases by 14% between 30 and 60°C (Figure 2H). Because ΔG_r decreases as a function of temperature, this observation is solely explained by the increased NGAM energy requirements at the higher temperature, as predicted by Tijhuis et al., (1993; Figure S1A,B). The product yields remain largely unchanged, with only a slight 1% increase between 30 and 60°C, while the biomass yields decrease by 5–13% over the same range because of the increased maintenance requirement (Figure 2G). Therefore, increasing temperature steers substrate towards increased product formation, by favouring acetate over biomass production. The product to biomass ratio increased by 6% in carboxydotrophs and by 14% in hydrogenotrophs between 30 and 60°C. It should be noted that this result is based on simplified metabolic energy demands that would require experimental confirmation. Studies on the effect of temperature on production to biomass yields of mixed acetogenic cultures, and on the metabolically closely related methanogens do confirm these predictions (Böske et al., 2015).

The yield calculations show the maximum achievable theoretical yields based on thermodynamics, where in practice yields would be lower. Cells are limited in their energy generation capacity by intermediate molecules such as ATP or through ion gradients, thus lowering the achieved yields. Different acetogenic organisms differ in their energy and redox metabolisms (Katsyv & Müller, 2020), regardless of their optimum growth temperature. Considering evolution and selection favours species that have efficient energy metabolism and hence growth at their given temperature optima, the experimental product and biomass yields would nevertheless follow the observed trend.

Process simulation

To investigate the effect of the calculated yields and maintenance requirements in the BCR setup, whilst also accounting for the changing gas mass transfer rates, the black box model of acetogenic metabolism was included in a simulated BCR at both 30 and at 60°C (Figure 3). In this simulation, the process is simplified by assuming a continuous product recovery, keeping acetate concentration in the liquid at zero. This assumption is necessary to investigate the steady state of a continuous production process, unhindered by product inhibition. In situ product removal can be achieved through classical separation techniques such as liquid–liquid extraction (Katikaneni & Cheryan, 2002), by using membranes (Gössi et al., 2020), or by converting the produced acetate into other, more easily separable products, such as VOCs in a coupled secondary fermentation (Bäumler et al., 2021). A process presents many operation parameters that can be fine-tuned. For BCRs, volume, height-to-diameter ratio, flow rate, bubble size and feed gas composition are key parameters. With all but the last already defined in the initial reactor setup, the main parameter left to define is the feed gas composition. As a starting point, only hydrogenotrophic acetogenesis is considered in the simulation. If the gasses were fully dissolved, the ideal feed composition would be the same as the stoichiometric uptake ratio, namely 2:1 (H_2:CO_2). However, since the transfer rate of CO_2 is an order of magnitude higher, H_2 must be fed at greater amounts. To investigate this, we model the steady-state outcome as a function of the mol fraction of H_2 in the feed gas (Figure 3A,B). The predicted optimal gas composition is then used as an input for following simulations.

In the steady-state comparison (Figure 3A) the maximum reachable biomass initially increases with increasing H_2 mol fraction, until it abruptly drops between 80 mol % and 90 mol %. At these points the H_2 is no longer the limiting substrate, as CO_2 becomes limiting. To compare how the increased H_2 mol fraction in the feed gas is reflected in the off gas, another steady state analysis is done (Figure 3B). Because the percentage of H_2 consumed from the feed gas, i.e. 30.7% at 30°C and 44.7% at 60°C, remains unchanged up to that point (Figure 3B), it is optimal to choose a gas composition as close as possible to this ratio, much closer to 9:1 (90 mol %) than to the stoichiometric 2:1 ratio (67 mol %). The exact values are found to be 0.86 mol % at 30°C and 0.81 mol % at 60°C, which are used for the respective gas compositions of the following simulations. It is noteworthy that, at 30°C, the predicted maximum achievable biomass concentration reaches cell densities so high that they would increase fluid viscosity, which in turn decreases the k_La and accordingly, the transfer rates. Overall, high cell density is to be avoided in BCRs for this reason, which is also an argument in favour of a thermophilic process (Heijnen & Van't Riet, 1984). When considering CO fermentation, CO is the sole gaseous substrate, so the optimum feed is 100% CO. Fermentations with mixed feeds containing CO as well as CO_2, and H_2 have no defined optimum but would range between the two optima: 1:0:0 and 0:9:1, keeping in mind that carboxydrotrophic growth produces CO_2, decreasing the required CO_2

17517915, 2024, 2, Downloaded from https://ami-journals.onlinelibrary.wiley.com/doi/10.1111/1751-7915.14414 by Danish Technical Knowledge, Wiley Online Library on [23/02/2024]. See the Terms and Conditions (https://onlinelibrary.wiley.com/terms-and-conditions) on Wiley Online Library for rules of use; OA articles are governed by the applicable Creative Commons License

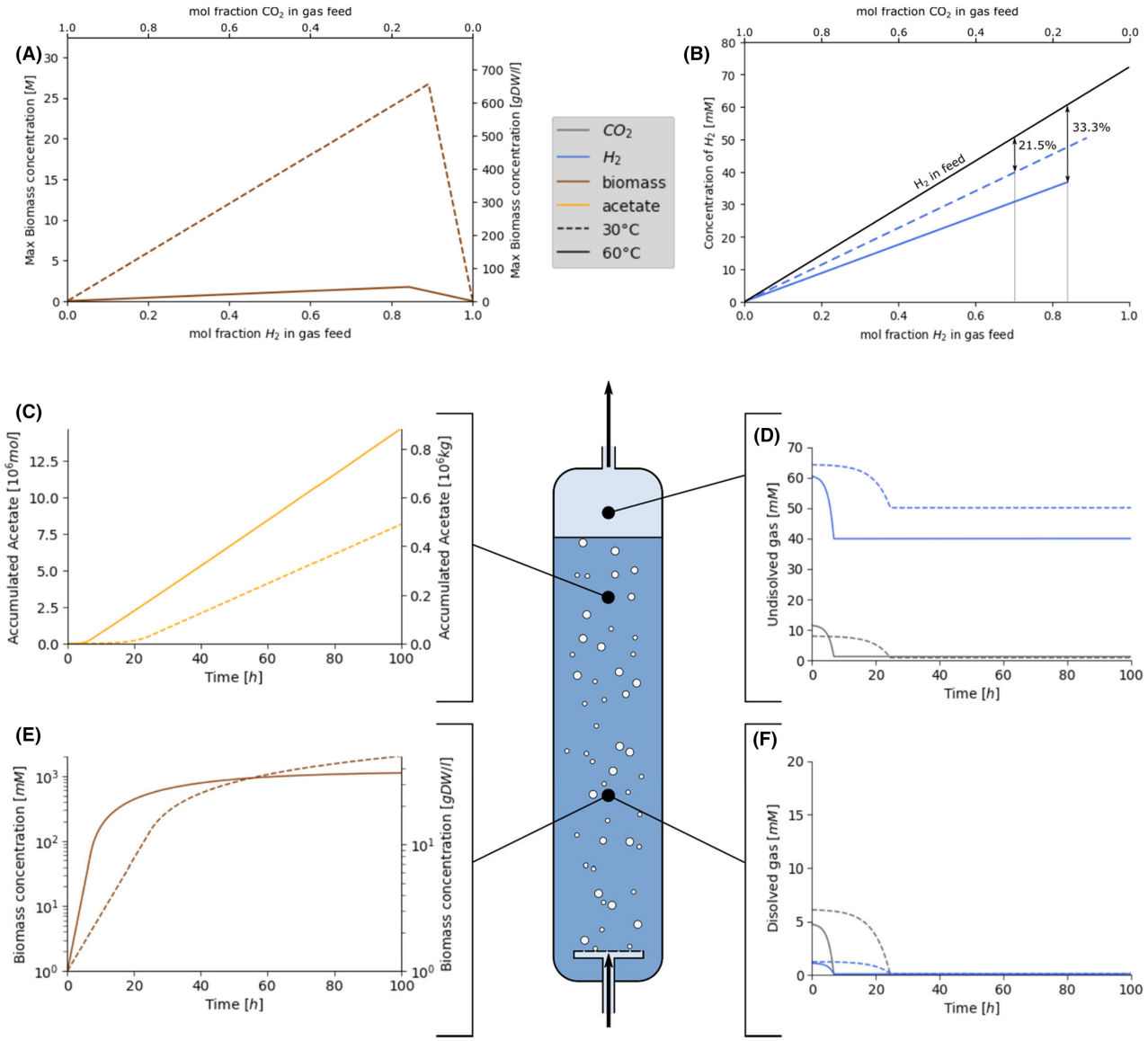

FIGURE 3 Steady-state analysis for optimal gas composition (A, B) to find the maximal reachable biomass concentration (A) and the ratio of H_2 consumed from the feed (B) as functions of the mol fraction of H_2 in the feed gas. The optimal gas composition is then used for a simulation of acetogenic growth in the described BCR at 30 and 60°C (C–F) with continuous product removal. The results are split into accumulation of the product, acetate (C), undissolved gasses in the gas phase and off-gas (D), biomass concentration (E) and dissolved gasses in the fermentation broth (F). In all plots dashed lines show simulations at 30°C and plain lines at 60°C.

feed concentration even further. The optimum would need to be calculated for the available feed gasses and depends on economics more than on mass transfers.

With the gas-fed, batch reactor simulations at 30 and 60°C, temperature effects on yields, biological rates and transfer rates can be calculated (Figure 3C–F). Initially, dissolved gasses are at saturation concentrations, which are higher at lower temperatures, however, they begin to decrease as the cells grow (Figure 3F). A pseudo-steady state is reached where the mass transfer of H_2 becomes limiting, keeping the concentration of dissolved gasses at 0 mM. During this pseudo-steady state, the concentration of undissolved gasses is lower at 60°C, meaning that more gas is converted and less is wasted through the off-gas (Figure 3D). From a biological point of view, initial growth rates are at their theoretical maxima, which are higher at 60°C. However, when gas transfer becomes limiting, the growth rate gradually decreases and the cells at the 30°C condition would slowly grow to higher densities than those at 60°C (Figure 3E). Maintenance energy requirements increase with temperature and energy is generated by acetate production; less biomass can thus in theory be sustained at 60°C. The product formation rates on the other hand remain constant (Figure 3C), with 0.88 and 1.5 tons of acetate being produced in the reactor per hour at 30 and 60°C respectively, corresponding to a specific productivity of 1.56 and 2.68 kg acetate per m^3 per hour. Overall, the simulations predict 1.7-fold higher production rates at 60°C. These amounts are in a

17517915, 2024, 2, Downloaded from https://ami-journals.onlinelibrary.wiley.com/doi/10.1111/1751-7915.14414 by Danish Technical Knowledge, Wiley Online Library on [23/02/2024]. See the Terms and Conditions (https://onlinelibrary.wiley.com/terms-and-conditions) on Wiley Online Library for rules of use; OA articles are governed by the applicable Creative Commons License

comparable range to the estimate by Redl, Sukumara, et al. (2017). of 3.79 tons of acetone produced per hour in the same reactor setup (Redl, Sukumara, et al., 2017). A decreasing biomass formation combined with a higher product formation pushes towards higher product on biomass yields at higher temperatures. These two simulations support the previous findings, thereby confirming that the transfer rate of a gas is more influential than its saturation concentration. Additionally, higher maintenance requirements at 60°C result in an advantageously higher yield of product per biomass and production rates that are almost doubled.

Product comparison by stoichiometric modelling of the WLP

As the data thus far shows, temperature greatly affects the gas fermentation process, leading to advantageous properties of thermophilic production for catabolic products, specifically for CO_2 utilisation. To develop a platform technology for CO_2 consumption, modular production of various products of interest at high yield should be considered. Additionally, insightful perspectives on the metabolism of acetogenesis can be gained when comparing acetate production to various other possible products. Several studies show the heterologous expression of genes allowing for acetone and isopropanol production derived from acetyl-CoA by acetogens themselves (Berzin et al., 2012; Daniell et al., 2012; Hoffmeister et al., 2016; Kato et al., 2021; Liew et al., 2022; Pogrebnyakov & Nielsen, 2021), expanding the list of small compounds that are innately produced by acetogens. With the constant development of synthetic biology tools, expanding this to thermophilic acetogens has become possible (Kato et al., 2021), though difficult and time-consuming. Considering that the WLP is an energy demanding pathway relying on product formation for its energy, we investigated which common bulk biochemicals are energetically favourable metabolites to produce and thus suitable targets.

The simplest method to compare the thermodynamic feasibility of acetogenic carbon utilisation into each of these various products is by calculating the difference in ΔG_r. The reaction stoichiometry and ΔG_r were calculated for a range of possible products in the same way as for the black box model of acetogenesis (Figure 4B, Table S2). Products considered are derivatives of acetate or acetyl-CoA, namely: ethanol, butanol, acetone, butyrate and butanediol. Interestingly, all selected products have similar ΔG_r. To determine for each product how much of that ΔG_r is usable for the cell's metabolism, a stoichiometric pathway model, focusing on the energy and redox intermediates was constructed (Figure S3). The metabolic map can be divided around its core metabolite acetyl-CoA, yielding the upstream WLP and downstream product formation (Figure 4A). To deduce the overall stoichiometry for each of the substrate and product combinations, the carbon incorporation to acetyl-CoA and the following product formation can be summed up. Accordingly, acetate and ethanol are the only products that fully restore the ATP consumed upstream to produce acetyl-CoA through their downstream metabolism, directly from substrate level phosphorylation (Figure 4A, stoichiometric sums in Table S1). Acetone and butyrate restore half, whereas butanol and butanediol do not generate any ATP. While ATP is the main biological energy carrier, energy can also be stored in redox intermediates such as NADH, NADPH or ferredoxin, or as sodium or proton gradients across the cell membrane, which can be converted to ATP through a sodium- or proton-driven ATP synthase. Although central

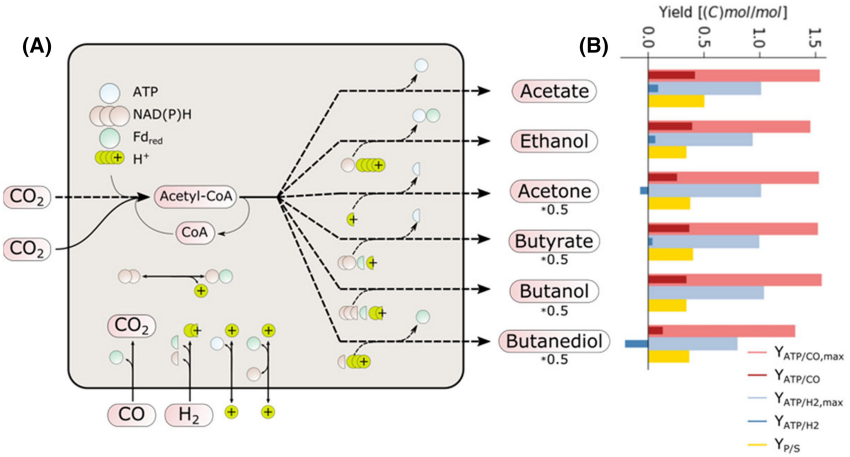

FIGURE 4 Product comparison by metabolic pathway analysis of the WLP showing a simplified pathway map of the WLP and its various products (A), and the ATP and product yields for different acetogenic products (B), as predicted by reaction thermodynamics (light blue and red) and how much of that theoretical maximum is stored in ATP as predicted by the stoichiometric model (dark blue and red). The product per substrate yields (yellow) is a metric for how much product is formed per mol electron source used. ATP yields are shown in mol/mol, whereas product yields are shown as Cmol/Cmol.

17517915, 2024, 2, Downloaded from https://ami-journals.onlinelibrary.wiley.com/doi/10.1111/1751-7915.14414 by Danish Technical Knowledge, Wiley Online Library on [23/02/2024]. See the Terms and Conditions (https://onlinelibrary.wiley.com/terms-and-conditions) on Wiley Online Library for rules of use; OA articles are governed by the applicable Creative Commons License

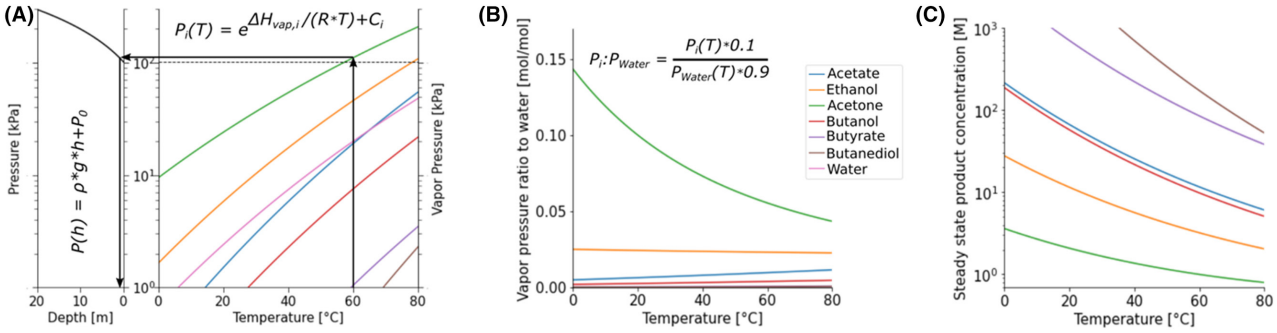

FIGURE 5 Analysis of volatile product recovery, represented through investigation of the vapour pressures of selected pure solutions of VOCs as a function of temperature (A, right), juxtaposed to the increase of pressure as a function of depth in the reactor (A, left). The arrows show how both can jointly be read to find the reactor depth at which a chosen compound reaches its boiling point for any reaction temperature. The ratio of vapour pressure of VOC to water in the off gas, for biologically relevant concentrations of 1% mol fraction VOC in aqueous broth determined across a temperature range (B). The product concentration in the bulk of the BCR at steady state as a function of temperature, based on the mass transfer models and overall reaction stoichiometry (C).

to the cell's metabolisms, these differ fundamentally between acetogenic species (Katsyv & Müller, 2020). For some acetogenic species, these mechanisms have been well defined. *C. ljungdahlii*, which was used as a template for the stoichiometric model, uses three of these enzyme complexes. To form ATP from a proton gradient over the cellular membrane, it uses a proton-driven ATP synthase. Additionally, ferredoxin NADH-linked hydrogenase splits H_2 to reduce ferredoxin and NAD^+. Lastly, Ferredoxin:NAD^+ Oxidoreductase (Rnf) allows NAD/NADH to reduce ferredoxin and vice versa, also using the proton gradient as a driving force. When including these reactions in the stoichiometric model, the proton and redox factor requirements or production of the metabolic reactions can be translated to ATP generation only, which determines whether the pathways can generate energy for cellular growth (Figure 4B, Table S2).

When comparing potential fermentation products, two metrics are especially important. Firstly, the ATP yield on the electron donor determines how much energy the cells can generate for both growth and maintenance. Secondly, the product yield quantifies how much product is formed per electron donor. In general, carboxydotrophic growth has higher yields than hydrogenotrophic growth. Additionally, a rough trend of decreasing yields with increasing product size can be observed, with acids having higher yields than alcohols. Acetate stands out through both its ATP and product yield. Compared to ethanol, which is a downstream product of acetate, it is more beneficial for two reasons. Firstly, the reaction of acetate to ethanol through acetaldehyde requires two reducing equivalents. Secondly, the acetate proton symporter feeds the proton motive force in a wide range of organisms, including acetogens (Boenigk et al., 1989). The proton motive force can power ATP synthase and, in some acetogens including *C. ljungdahlii*, the bifurcating enzymes such as Rnf. Butanediol gives the lowest ATP yield, requiring ATP to utilise CO_2 as a substrate. Acetone is also energetically unfavourable, requiring ATP to be produced from CO_2. An alternative acetone production pathway has recently been proposed, which directly generates ATP by using a phosphate butyryltransferase and a butyrate kinase enzyme that will promiscuously catalyse the transformation of acetoacetyl-CoA to acetoacetate, through acetoacetyl-P (Tschaplinski & Simpson, 2019). However, when including this pathway in the stoichiometric model and comparing the yields to the pathway from *C. acetobutylicum*, the same overall yields are observed, meaning that the pathways are energetically equivalent (Figure S4). Negative or neutral ATP yield values do not mean that the products cannot be formed, but that flux towards another product that does generate energy is required to supply the required energy for both production and growth. This is also a common phenomenon when strains are heavily engineered past energetic limits to force formation of a specific product, resulting in significant byproduct formation to meet cellular energy and redox demands.

The stoichiometric model builds on a steady state assumption, so all accumulations except substrate, product and ADP/ATP are set to be zero. In vivo, the redox intermediates NADH, NADPH and ferredoxin are involved in other parts of cellular metabolism. Modelling a steady state pushes flux through the bifurcating enzymes, which could affect ATP yields. Therefore, one should be cautious when determining a clear cut-off value for the feasibility of producing compounds. Nonetheless, the combined properties of acetate, having both a high ATP and product yield make it a suitable candidate for acetogenic carbon utilisation. Evolutionary pressure will push for its stable production, and its production results in the most carbon being utilised.

Volatile product comparison for in situ recovery

Having demonstrated that thermophilic fermentations are theoretically beneficial for the uptake and conversion of gaseous substrates, one can also consider

17517915, 2024, 2, Downloaded from https://ami-journals.onlinelibrary.wiley.com/doi/10.1111/1751-7915.14414 by Danish Technical Knowledge, Wiley Online Library on [23/02/2024]. See the Terms and Conditions (https://onlinelibrary.wiley.com/terms-and-conditions) on Wiley Online Library for rules of use; OA articles are governed by the applicable Creative Commons License

another advantage of increased temperature, specifically the possibility of in situ removal of volatile products of interest through the off-gas. This enables more simplified downstream processing, prevents product toxicity to production strains and feedback inhibition on production pathways, overall leading to higher specific productivities of a process. Low boiling point derivatives of acetate, such as acetone, previously produced as a product of the WLP (Kato et al., 2021), are possible products to consider. Evaporation can happen either by gas stripping, which depends on its vapour pressure, or by boiling, which happens when the vapour pressure exceeds the ambient pressure. Thus, the vapour pressures of selected volatile compounds were expressed as a function of temperature for a range of possible products (Figure 5A). Of all modelled compounds, acetone is the most volatile, followed by ethanol, with vapour pressures pushing the boiling point below 60 and 80°C at atmospheric pressure respectively (Figure 5A). Other products around or below the vapour pressure of water. However, the pressure in the reactor is not atmospheric as it varies significantly by the depth in the broth, especially for tall BCRs (Figure 5A). From here, one can observe the depth at which the pure compound of interest will boil at the given temperature. Assuming a process temperature falling within the physiologically relevant 30 and 70°C range, evaporation by boiling would only occur for pure acetone in a fraction of the reactor around or above 60°C.

Additionally, in a biological fermentation process where cells are suspended in liquid media, one would expect an aqueous broth with product concentrations at a maximum of 5–10% (w/v), in part due to product inhibition and toxicity (Fan et al., 2018; Pierce et al., 2008; Zhang et al., 2020). In an aqueous solution, both the boiling point of the solution and the vapour pressure of the solute change. The change in the boiling point of a mixture depends on complex physicochemical interaction properties of the solvent and solute, which must be experimentally determined. For the example of acetone, studies have experimentally measured these values for aqueous mixtures at varying mol fractions and pressures and identified that the boiling point of the mixtures starts at that of pure acetone, remains relatively flat until a 10% acetone mol fraction, and then steeply increases to the boiling point of pure water (Othmer et al., 1952). In a BCR setting, even at thermophilic temperatures, boiling is thus likely insufficient to allow effective product recovery. Yet, even below the boiling point, the VOC can still diffuse to the gas phase through the exerted vapour pressure. Gas stripping could therefore provide a second evaporative mechanism for in situ product recovery. As with boiling, this needs to be corrected for the mole fraction of the product in the solution. In solution, the partial vapour pressure can linearly be related to the molar fraction of the compound and the vapour pressure of the pure component through Raoult's law. For acetone, the most volatile and hence favourable compound, assuming a biologically relevant mol fraction of 1% (corresponding to a relatively high concentration of approximately 0.6 mol/L or 32 g/L), the vapour pressure would be 1% of that of the pure solution, pushing it far below that of water. Hence, at a given temperature, the ratio of VOC to water that will evaporate, at steady state, equals the vapour pressure of the solute divided by that of the whole solution (Figure 5B). With higher temperature, the ratios change as the vapour pressures of the different compounds change independently. The vapour pressure of water increases more steeply with temperature than most dilute VOCs (Figure 5A). In the example of a 1% solution of acetone, the ratio decreases from 7.6 to 5.5% (Figure 5B) between 37 and 60°C, but still corresponds to a 7.6 and 5.5-fold enrichment of the VOC from the liquid to the gas.

The feasibility of volatile product recovery relies on the ability of the gas stripping to push down the product concentration to avoid inhibitory effects and allow continuous production. We thus chose to investigate for the given BCR at the given feed rate, whether the exerted vapour pressure is sufficient to keep the product concentration low (Figure 5C). At a steady state with continuous production, there is no product accumulation, so product removal rate must equal the production rate. Equally, at steady state, the biomass concentration has reached its maximum, thus all H_2 consumed goes to the product. Therefore, the production rate is a direct function of the H_2 consumption rate, which equals the H_2 mass transfer rate at steady state. Similarly to the gas–liquid mass transfer rate analysis, the concentration of dissolved H_2 is assumed to be zero. Using both the substrate mass transfer rate and the overall reaction stoichiometries, the maximum product formation rates are calculated for each product. Assuming that the product concentration in the off-gas reaches its saturation, the concentration in the bulk is in equilibrium with the concentration in the gas, as dictated by the vapour pressure and the gas volume and flow rate, which is assumed to equal the inflow to satisfy the steady state assumption, meaning in practice that we assume that the gasses taken up are replaced by evaporating water and products. The two products with the lowest predicted concentrations are ethanol and acetone. At 60°C, ethanol is predicted to reach a concentration of 3.2 M (147.2 g/L), while acetone reaches 1.0 M (57.8 g/L). Only acetone comes to a biologically relevant 5–10% w/v product concentration range. However, tolerance is highly host specific, and only once a host is selected is it possible to confirm the tolerance levels. If needed, tolerance can be improved with strain engineering or laboratory evolution (Sandberg et al., 2019). As opposed to the two-film theory model used for the absorption

17517915, 2024, 2, Downloaded from https://ami-journals.onlinelibrary.wiley.com/doi/10.1111/1751-7915.14414 by Danish Technical Knowledge, Wiley Online Library on [23/02/2024]. See the Terms and Conditions (https://onlinelibrary.wiley.com/terms-and-conditions) on Wiley Online Library for rules of use; OA articles are governed by the applicable Creative Commons License

model, the product removal calculations are built only on steady-state concentrations dictated solely by the compound's vapour pressures. It is not tested whether a steady state is reached and the gas is saturated before it leaves the reactor. This implies that the molar percentage of product in the off-gas could be higher if the transfer rate of the product is higher than that of water.

In conclusion, while operating above the boiling point of the pure product does not guarantee successful in situ product removal, gas stripping could be sufficient to continuously recover acetone in a BCR setup at thermophilic conditions and keep a concentration within a biologically relevant range. There is no clear temperature threshold above which the recovery becomes feasible, rather, the higher the temperature, the lower the steady state product concentration is and the less product inhibition affects the process. Inevitably, continuous product evaporation will also evaporate large amounts of water, which forms a challenge for the process design and operation.

DISCUSSION

Microbial gas fermentation is an efficient platform that enables the conversion of CO_2-rich waste gas streams into biomass and organic carbon compounds, which can be used as sustainable products. To harness this power, optimisation of both the production strain and process are critical to achieve sufficiently high efficiencies and productivities, to outcompete petrochemical production in the economic-incentive-driven society.

Applying host-agnostic mechanistic models allows for tailored selection of microbial hosts based on final process requirements. Particularly advantageous to using host-agnostic black box modelling is the low dependency on large a priori experimental datasets, which are often not available when pushing the boundaries of novel production processes and microbial phenotypes. In this way, a more efficient allocation of resources can be achieved when process and metabolic modelling are used to narrow the solution space that must be experimentally probed. Requiring limited data input, this approach offers a modular platform to explore novel bio-manufacturing possibilities, moving the field away from traditional production organisms and processes. While the presented findings are purely based on modelling results, all modelling in this work builds on well-established concepts that have been meticulously documented in literature. Indeed, the gas transfer rates and vapour pressure calculations are basic concepts that are commonly used in process engineering, as referenced in the methods section. Similarly, the stoichiometric model of acetogenic metabolism is the product of meticulous research of acetogens and their Wood-Ljungdahl pathway. While the temperature correction of the maximum growth rate and the NGAM has not been used in the field of process design, the underlying phenomenon is widely accepted in other fields including ecology and food preservation, where NGAM would be described as the death rate. Although such modelling approaches are advantageous to limit the experimental test space, they can fall short of capturing intricate processes, either because they are a simplification of complex systems or because certain factors are unknown. The sole purpose of this analysis is to qualitatively compare the effect of temperature on gas fermentations and investigate which products can be formed. Therefore, looking forward, critical biological and experimental aspects presented here should be considered and tested in future work, to allow for accurate simulations. From a process engineering perspective the effect of media components and products in the bulk on the gas transfer rates and evaporation rates must be determined. From a biological perspective, the actual biological rates of growth and substrate uptake need to be measured, as well as the maintenance energy requirements and the inhibition of the various compounds. Nonetheless, this modelling approach has been demonstrated here to be a valuable tool to narrow down the experimental test space and could be applied to query other unconventional types of metabolism, such as the many other types of anaerobic respiration (Lovley & Coates, 2000).

We show that for catabolic products, product yields increase with temperature due to the higher demand for maintenance energy. Specifically, for acetogenesis, metabolic modelling performed here shows that the energetic feasibility of acetogenesis depends solely on the downstream metabolism of product formation, to compensate the energy-demanding WLP, with acetate being the most energetically favourable product whilst also utilising the most carbon per electron donor. Ethanol is also a suitable product, although it requires more H_2 because it is more reduced. However, producing ethanol comes with major advantages compared to acetate, which make it an interesting product nonetheless. As demonstrated in the volatile product recovery calculations, ethanol can more easily be recovered from the broth. Additionally, acetate production continuously acidifies the broth, requiring pH adjustment leading to salt formation, which is not a problem in ethanol formation. When other products than acetate or ethanol are desired, lower yields would be achieved, as by-product formation is required for energy generation. This is often what is observed in gas fermenting organisms (Bengelsdorf et al., 2016; Jia et al., 2021), resulting in more complex downstream processing and overall lower titres.

While most claims for the benefits of thermophilic processes have been put to the test in the presented analyses, the contamination risk and lower cooling cost have not been addressed. Indeed the

17517915, 2024, 2, Downloaded from https://ami-journals.onlinelibrary.wiley.com/doi/10.1111/1751-7915.14414 by Danish Technical Knowledge, Wiley Online Library on [23/02/2024]. See the Terms and Conditions (https://onlinelibrary.wiley.com/terms-and-conditions) on Wiley Online Library for rules of use; OA articles are governed by the applicable Creative Commons License

surrounding mesophilic environment of the reactor is a barrier for the simple reason that it contains few thermophilic contaminants, however, contaminants can also come from the feed, which, depending on the origin of the gas can also be a thermophilic environment. Moreover, contaminants become increasingly an issue as they outperform the production strain, one could argue in the case of acetogens that their main contaminant, methanogens, should outperform them at higher temperatures because of the Gibbs free energy of reaction becoming increasingly favourable with temperature (Figure S1A). Additionally, for production hosts producing a compound that is not their favoured catabolic product (e.g. all products besides acetate and ethanol here), the "contaminant" could come from the inoculum itself, through cells that loose the production pathway under selective pressure. Since thermophiles have an increased energy requirement of NGAM, this selective pressure is increased. Therefore, although there is a significant benefit of operating at higher temperature, there is still a risk of contamination. Regarding the reactor cooling cost, the overall chemical reactions remain exogenic, meaning that the same amount of heat needs to be removed from the reactor. While there might be more evaporation from the broth cooling the reactor, the main advantage is that the temperature difference between a thermophilic fermentation and its surroundings is such that water at room temperature cooler can be used, while a mesophilic fermentation would require the cooling liquid to be cooled, thereby making the cooling significantly more costly.

Using mass transfer models and process simulations, we have investigated improved operating conditions for a BCR. We demonstrate in this study that higher temperatures are beneficial for gas uptake rates, essential for substrate availability in acetogenesis, while to date predominant industrial work with gas fermentation is performed in the mesophilic temperature range (Vees et al., 2020). While BCRs are a good starting point for gas fermentations due to their simplicity, scalability and low maintenance (Noorman & Heijnen, 2017), more complex and costly reactor types can also be envisioned if their properties address the shortcomings of BCRs. To our knowledge, there is currently no quantitative comparison of reactor performance between setups for the specific purpose of acetogenic gas fermentation. Such a study could provide valuable insights and further improvements into gas fermentation-mediated CO_2 upcycling. Mass transfer models based on experimental data of continuous stirred tank (CSTR) (Liu et al., 2019), packed bed (PBR) (Steger et al., 2022) or external loop airlift (ELAR) (Puiman et al., 2022) reactors have been published. Especially the latter two reactor types are worth considering because of their potential to improve gas transfers (Nikakhtari & Hill, 2005). The packing of PBRs holds up and breaks up gas bubbles increasing gas mass transfer rates through both an increased total gas phase volume and a larger surface area (Nikakhtari & Hill, 2005). The packing can also serve as a support for immobilised cells, allowing for higher cell concentration and retaining the cells in the reactor, which allows for medium exchange and eases downstream processing (Pörtner & Faschian, 2019). ELARs are designed to have two columns, a riser column that is pushed up by the gas feed, and a downcomer recirculating the broth. With this design, the gas flow is used to circulate broth through the reactor, with each column functioning as a plug-flow reactor. The broth entering the riser, having the lowest dissolved gas concentration, is exposed to the highest partial gas pressures, making for increased transfer rates. While the BCR can only be optimised by changing the reactor size, height-to-width ratio, gas flow and bubble size, PBRs and ELARs have more parameters that can be optimised, such as the packing type and pore size, or the riser to downcomer size ratio. Additionally, aspects from each reactor can be combined, for example, an ELAR can be designed with a packed bed and stirring. While these comparisons are not included in the present work and future work could focus on quantifying these effects and optimising the process, the main findings of this paper can be generalised to gas fermentation in any of these reactor designs. Indeed, with solely gaseous substrates, gas transfer is expected to be limiting regardless of the reactor type. Considering that the main difference between the reactor setups from a mass transfer perspective is the value of $k_L a$ (Doran, 2013), the findings of this research can also be applied to other reactor types.

Gas transfer rates are only limiting as long as the fermentation is substrate limiting. If, through product accumulation, growth becomes product inhibited, product removal becomes the bottleneck. Then, in situ product removal can greatly benefit specific productivities. However, our calculations predict that product removal is only within reach for acetone and comes with the challenge of predicted dilute concentrations in the recovered gas, due to the large amounts of water evaporating. Other studies have also highlighted this challenge for other types of fermentation processes such as ABE fermentation (Díez-Antolínez et al., 2018; Li et al., 2016; Liao et al., 2014; Rochón et al., 2017; Schiel-Bengelsdorf & Dürre, 2012; Wen et al., 2018; Xue et al., 2016). When comparing the thermophilic gas fermentation to these mainly mesophilic ABE fermentations, the former comes with the advantage of gas feed already serving as the stripping gas, while the ABE fermentation uses a dissolved substrate, meaning that a separate stripping gas needs to be used, adding to the process complexity and operation cost. Additional processing steps can help the purification of the volatile product. The simplest addition is a second distillation after condensation of the off-gas, possibly using high osmolarity to salt out

17517915, 2024, 2, Downloaded from https://ami-journals.onlinelibrary.wiley.com/doi/10.1111/1751-7915.14414 by Danish Technical Knowledge, Wiley Online Library on [23/02/2024]. See the Terms and Conditions (https://onlinelibrary.wiley.com/terms-and-conditions) on Wiley Online Library for rules of use; OA articles are governed by the applicable Creative Commons License

the product (Wen et al., 2018). This is however purely downstream and does not affect the product concentration in the broth. If experimental work would show that the concentration needs to be pushed even lower, an option would be to increase the gas flow by adding a stripping gas. Increasing the overall gas flow in a BCR can break the flow of the air bubbles and cause a relative decrease of $k_L a$ (Heijnen & Van't Riet, 1984), therefore the feed rate can be kept the same while changing the gas composition to include N_2 or more CO_2. More elaborate in situ product removal methods that do not rely on evaporation can also be considered, such as the use of membranes (Gössi et al., 2020) or polymeric resins (Nielsen & Prather, 2009) that separate the product based on other physiochemical properties, such as polarity. These are much more complex and come with a whole new set of challenges, especially when used in the relatively dirty environment of a fermentation.

Overall, a BCR enables high gas absorption rates with minimal operation complexity and costs. Increased operation temperature favour both gaseous substrate uptake and formation rates and yields of catabolic products. Energy generation in acetogenic gas fermentation relies on product formation, with acetate being by far the favoured product. However, acetate is a product of limited value that cannot be recovered in situ by gas stripping. To reconcile this with the found benefits of a thermophilic gas fermentation in a BCR, several strategies can be considered. A co-substrate could be added to expand the product range. Other products could be formed by acetogenesis despite their yields being less suitable, most likely producing a mixture of compounds. Acetate could be used as an intermediate metabolite for further conversion into more valuable compounds, either by chemical catalysis or by a second fermentation step by a heterotrophic production host.

Taken together, this work highlights how the interplay of process and metabolic modelling can be used to steer bioprocess design to harness novel phenotypes and to allow probing of process parameters such as temperature and feed composition. Starting from the final production aim, we work our way back to choose suitable reactor operation conditions and a fitting production host. Specifically, the temperature-dependent, host-agnostic growth model is a powerful novel tool to assess and compare possible production hosts when the reactor conditions are not yet known. Combined with mass transfer models and metabolic pathway analysis into a process simulation, this approach has allowed to quantitively compare fermentation conditions and narrow down the range of process possibilities. Here, the study is specifically applied to microbial CO_2 fixation, aiming to assess the technology and push it further with the aim of providing a new tool to battle one of the most pressing global issues. Overall, this pushes the paradigm to rely less on conventional production organisms and organic carbon substrates, highlighting the possibility of efficiently converting gaseous waste streams into valuable chemicals, needed to achieve the ambitious climate goals society has set.

Nomenclature

a area [m^2]

c concentration (c*: saturation c, c_P* limiting inhibitory c) [mM]

D diffusion coefficient [m^2/s]

F flow rate [m^3/h]

g acceleration of gravity [m/s^2]

H Henry's law constant [mol/m^3*Pa]

h height [m]

k coefficient or constant, defined per case

m_{GAM} GAM energy requirement [$kJ/mol_{biomass}$]

m_{NGAM} NGAM energy requirement [$kJ/h/mol_{biomass}$]

P (vapour) pressure (P_m: mean logarithmic, P_b: bottom, P_t: top, P*: partial) [Pa]

q specific consumption or production rate [h^{-1}]

R gas constant [$m^3*Pa/K/mol$] or R Transfer rate [$mol/m^3/s$]

r radius [m]

T temperature [K]

V volume [m^3]

v^c_{gs} superficial gas velocity [m^3/h]

v stoichiometric factor [unitless]

x mol fraction [mol/mol]

Y yield (PS: product on substrate, XS: biomass on substrate, …) [(C)mol/(C)mol]

$\Delta H_{r/f/vap}$ enthalpy of reaction/formation/vaporisation [kJ/mol]

$\Delta G_{r/f}$ Gibbs free energy of reaction/formation [kJ/mol]

ε gas holdup fraction [unitless]

θ temperature correction factor of $k_L a$ [unitless]

17517915, 2024, 2, Downloaded from https://ami-journals.onlinelibrary.wiley.com/doi/10.1111/1751-7915.14414 by Danish Technical Knowledge, Wiley Online Library on [23/02/2024]. See the Terms and Conditions (https://onlinelibrary.wiley.com/terms-and-conditions) on Wiley Online Library for rules of use; OA articles are governed by the applicable Creative Commons License

μ specific growth rate [/h]

π pi [unitless]

ρ density [kJ/m^3]

Subscripts

i: compound I (or inhibition for K_i)
X: biomass

S: substrate

P: Product

max: maximum

ana: anabolic reaction

cata: catabolic reaction

G: in the gas phase

L: in the liquid bulk

in: incoming (from feed flow)

T: at temperature T

0: at a specified reference condition

AUTHOR CONTRIBUTIONS

Philip J. Gorter de Vries: Conceptualization (equal); data curation (equal); investigation (equal); methodology (equal); visualization (equal); writing – original draft (equal); writing – review and editing (equal). **Viviënne Mol:** Conceptualization (equal); data curation (equal); visualization (equal); writing – original draft (equal); writing – review and editing (equal). **Nikolaus Sonnenschein:** Writing – review and editing (equal). **Torbjørn Ølshøj Jensen:** Conceptualization (equal); supervision (equal); writing – review and editing (equal). **Alex Toftgaard Nielsen:** Conceptualization (equal); funding acquisition (equal); project administration (equal); supervision (equal); writing – review and editing (equal).

ACKNOWLEDGEMENTS

We would like to thank Ivan Pogrebnyakov for fruitful discussions and support throughout the project. P.J.G.d.V. and V.M. are the recipients of a fellowship from the Novo Nordisk Foundation as part of the Copenhagen Bioscience Ph.D. Program, supported through grants NNF19CC0035454 and NNF18CC0033664 respectively. N.S. was funded by the Novo Nordisk Foundation within the framework of the Fermentation-based Biomanufacturing Initiative (FBM), grant number NNF17SA0031362. A.T.N. and T.Ø.J. received funding from the European Union's Horizon 2020 research and innovation programme under grant agreement number 101037009 (PyroCO2). We further acknowledge funding from the Novo Nordisk Foundation (grant number NNF20CC0035580), the Villum Fonden (grant number 40986) and the Danish Research Council (grant number 103200448B).

CONFLICT OF INTEREST STATEMENT

The authors declare that there are no competing interests associated with the contents of this article.

ORCID

Philip J. Gorter de Vries https://orcid.org/0000-0002-0311-5634
Viviënne Mol https://orcid.org/0000-0002-4401-686X
Nikolaus Sonnenschein https://orcid.org/0000-0002-7581-4936
Alex Toftgaard Nielsen https://orcid.org/0000-0001-6616-0187

REFERENCES

Bar-Even, A., Noor, E., Lewis, N.E. & Milo, R. (2010) Design and analysis of synthetic carbon fixation pathways. *Proceedings of the National Academy of Sciences of the United States of America*, 107, 8889–8894.

Bäumler, M., Schneider, M., Ehrenreich, A., Liebl, W. & Weuster-Botz, D. (2021) Synthetic co-culture of autotrophic *Clostridium carboxidivorans* and chain elongating *Clostridium kluyveri* monitored by flow cytometry. *Microbial Biotechnology*, 15, 1471–1485. Available from: https://doi.org/10.1111/1751-7915.13941

Bengelsdorf, F.R., Poehlein, A., Linder, S., Erz, C., Hummel, T., Hoffmeister, S. et al. (2016) Industrial acetogenic biocatalysts: a comparative metabolic and genomic analysis. *Frontiers in Microbiology*, 7, 1036.

Berzin, V., Kiriukhin, M. & Tyurin, M. (2012) Selective production of acetone during continuous synthesis gas fermentation by engineered biocatalyst *Clostridium* sp. MAceT113. *Letters in Applied Microbiology*, 55, 149–154.

Boenigk, R., Diirre, P. & Gottschalk, G. (1989) Carrier-mediated acetate transport in *Acetobacterium woodii*. *Archives of Microbiology*, 152, 589–593.

Böske, J., Wirth, B., Garlipp, F., Mumme, J. & Van den Weghe, H. (2015) Upflow anaerobic solid-state (UASS) digestion of horse manure: thermophilic vs. mesophilic performance. *Bioresource Technology*, 175, 8–16.

Brennan, T.C.R., Turner, C.D., Krömer, J.O. & Nielsen, L.K. (2012) Alleviating monoterpene toxicity using a two-phase extractive fermentation for the bioproduction of jet fuel mixtures in *Saccharomyces cerevisiae*. *Biotechnology and Bioengineering*, 109, 2513–2522.

Carnot, S. (1824) *Réflexions sur la puissance motrice du feu et sur les machines propres à développer cette puissance*. Paris, France: Bachelier.

Chen, C.-Y., Yeh, K.-L., Aisyah, R., Lee, D.-J. & Chang, J.-S. (2010) Cultivation, photobioreactor design and harvesting of microalgae for biodiesel production: a critical review. *Bioresource Technology*, 102(1), 71–81. Available from: https://doi.org/10.1016/j.biortech.2010.06.159

Cheng, C., Li, W., Lin, M. & Yang, S.T. (2019) Metabolic engineering of *Clostridium carboxidivorans* for enhanced ethanol and

17517915, 2024, 2, Downloaded from https://ami-journals.onlinelibrary.wiley.com/doi/10.1111/1751-7915.14414 by Danish Technical Knowledge, Wiley Online Library on [23/02/2024]. See the Terms and Conditions (https://onlinelibrary.wiley.com/terms-and-conditions) on Wiley Online Library for rules of use; OA articles are governed by the applicable Creative Commons License

butanol production from syngas and glucose. *Bioresource Technology*, 284, 415–423.
Clark, D.S. & Blanch, H.W. (1995) Bioreactor design and analysis. In: *Biochemical engineering*. Boca Raton: CRC Press.
Daniell, J., Köpke, M. & Simpson, S.D. (2012) Commercial biomass syngas fermentation. *Energies*, 5, 5372–5417.
Davey, K.R. (1993) Linear-Arrhenius models for bacterial growth and death and vitamin denaturations. *Journal of Industrial Microbiology*, 12, 172–179.
De Silvestri, A., Ferrari, E., Gozzi, S., Marchi, F. & Foschino, R. (2018) Determination of temperature dependent growth parameters in psychrotrophic pathogen bacteria and tentative use of mean kinetic temperature for the microbiological control of food. *Frontiers in Microbiology*, 9, 3023.
Díez-Antolínez, R., Hijosa-Valsero, M., Paniagua-García, A.I. & Gómez, X. (2018) In situ two-stage gas stripping for the recovery of butanol from acetone-butanol-ethanol (ABE) fermentation broths. *Chemical Engineering Transactions*, 64, 37–42.
Doran, P.M. (2013) Mass transfer. In: *Bioprocess engineering principles*. San Diego, CA: Elsevier, pp. 379–444. Available from: https://doi.org/10.1016/B978-0-12-220851-5.00010-1
Ebrahim, A., Lerman, J.A., Palsson, B.O. & Hyduke, D.R. (2013) COBRApy: COnstraints-Based Reconstruction and Analysis for python. *BMC Systems Biology*, 7, 74.
Fan, X., Wu, H., Jia, Z., Li, G., Li, Q., Chen, N. et al. (2018) Metabolic engineering of *Bacillus subtilis* for the co-production of uridine and acetoin. *Applied Microbiology and Biotechnology*, 102, 8753–8762.
Gassler, T., Sauer, M., Gasser, B., Egermeier, M., Troyer, C., Causon, T. et al. (2020) The industrial yeast *Pichia pastoris* is converted from a heterotroph into an autotroph capable of growth on CO_2. *Nature Biotechnology*, 38, 210–216.
Gössi, A., Burgener, F., Kohler, D., Urso, A., Kolvenbach, B.A., Riedl, W. et al. (2020) In-situ recovery of carboxylic acids from fermentation broths through membrane supported reactive extraction using membrane modules with improved stability. *Separation and Purification Technology*, 241, 116694.
Harris, C.R., Millman, K.J., van der Walt, S.J., Gommers, R., Virtanen, P., Cournapeau, D. et al. (2020) Array programming with NumPy. *Nature*, 585, 357–362.
Heijnen, J.J. (2010) Impact of thermodynamic principles in systems biology. *Advances in Biochemical Engineering/Biotechnology*, 121, 139–162.
Heijnen, J.J. & Van't Riet, K. (1984) Mass transfer, mixing and heat transfer phenomena in low viscosity bubble column reactors. *The Chemical Engineering Journal*, 28, B21–B42.
Hoffmeister, S., Gerdom, M., Bengelsdorf, F.R., Linder, S., Flüchter, S., Öztürk, H. et al. (2016) Acetone production with metabolically engineered strains of *Acetobacterium woodii*. *Metabolic Engineering*, 36, 37–47.
Huang, L., Hwang, A. & Phillips, J. (2011) Effect of temperature on microbial growth rate-mathematical analysis: the Arrhenius and Eyring-Polanyi connections. *Journal of Food Science*, 76, E553–E560.
Hunter, J.D. (2007) Matplotlib: a 2D graphics environment. *Computing in Science and Engineering*, 9, 90–95.
Ingraham, J.L. (1958) Growth of psychrophilic bacteria. *Journal of Bacteriology*, 76, 75–80.
Jia, D., He, M., Tian, Y., Shen, S., Zhu, X., Wang, Y. et al. (2021) Metabolic engineering of gas-fermenting *Clostridium ljungdahlii* for efficient co-production of isopropanol, 3-hydroxybutyrate, and ethanol. *ACS Synthetic Biology*, 10, 2628–2638.
Jouny, M., Luc, W. & Jiao, F. (2018) General techno-economic analysis of CO_2 electrolysis systems. *Industrial and Engineering Chemistry Research*, 57, 2165–2177.
Katikaneni, S.P.R. & Cheryan, M. (2002) Purification of fermentation-derived acetic acid by liquid-liquid extraction and esterification. *Industrial and Engineering Chemistry Research*, 41, 2745–2752.
Kato, J., Takemura, K., Kato, S., Fujii, T., Wada, K., Iwasaki, Y. et al. (2021) Metabolic engineering of Moorella thermoacetica for thermophilic bioconversion of gaseous substrates to a volatile chemical. *AMB Express*, 11, 59.
Katsyv, A. & Müller, V. (2020) Overcoming energetic barriers in acetogenic C1 conversion. *Frontiers in Bioengineering and Biotechnology*, 8, 1420.
Köpke, M., Mihalcea, C., Liew, F.M., Tizard, J.H., Ali, M.S., Conolly, J.J. et al. (2011) 2,3-Butanediol production by acetogenic bacteria, an alternative route to chemical synthesis, using industrial waste gas. *Applied and Environmental Microbiology*, 77, 5467–5475.
Krüger, A., Schäfers, C., Schröder, C. & Antranikian, G. (2018) Towards a sustainable biobased industry – highlighting the impact of extremophiles. *New Biotechnology*, 40, 144–153.
Lackner, K.S. (2003) A guide to CO_2 sequestration. *Science*, 300, 1677–1678.
Lee, H., Bae, J., Jin, S., Kang, S. & Cho, B.K. (2022) Engineering Acetogenic bacteria for efficient one-carbon utilization. *Frontiers in Microbiology*, 13, 865168.
Levenspiel, O. (1980) The monod equation: a revisit and a generalization to product inhibition situations. *Biotechnology and Bioengineering*, 22, 1671–1687.
Li, S.-Y., Chiang, C.-J., Tseng, I.-T., He, C.-R. & Chao, Y.-P. (2016) Bioreactors and *in situ* product recovery techniques for acetone–butanol–ethanol fermentation. *FEMS Microbiology Letters*, 363, fnw107.
Li, Y.J., Wang, M.M., Chen, Y.W., Wang, M., Fan, L.H. & Tan, T.W. (2017) Engineered yeast with a CO_2-fixation pathway to improve the bio-ethanol production from xylose-mixed sugars. *Scientific Reports*, 7, 43875.
Liao, Y.C., Lu, K.M. & Li, S.Y. (2014) Process parameters for operating 1-butanol gas stripping in a fermentor. *Journal of Bioscience and Bioengineering*, 118, 558–564.
Liew, F., Henstra, A.M., Köpke, M., Winzer, K., Simpson, S.D. & Minton, N.P. (2017) Metabolic engineering of *Clostridium autoethanogenum* for selective alcohol production. *Metabolic Engineering*, 40, 104–114.
Liew, F.E., Nogle, R., Abdalla, T., Rasor, B.J., Canter, C., Jensen, R.O. et al. (2022) Carbon-negative production of acetone and isopropanol by gas fermentation at industrial pilot scale. *Nature Biotechnology*, 40, 335–344. Available from: https://doi.org/10.1038/s41587-021-01195-w
Liew, F.M., Martin, M.E., Tappel, R.C., Heijstra, B.D., Mihalcea, C. & Köpke, M. (2016) Gas fermentation-a flexible platform for commercial scale production of low-carbon-fuels and chemicals from waste and renewable feedstocks. *Frontiers in Microbiology*, 7, 694.
Liu, K., Phillips, J.R., Sun, X., Mohammad, S., Huhnke, R.L. & Atiyeh, H.K. (2019) Investigation and modeling of gas-liquid mass transfer in a Sparged and non-Sparged continuous stirred tank reactor with potential application in syngas fermentation. *Fermentation*, 5, 75.
Lovley, D.R. & Coates, J.D. (2000) Novel forms of anaerobic respiration of environmental relevance. *Current Opinion in Microbiology*, 3, 252–256.
Masson-Delmotte, V., Zhai, P., Pirani, A., Connors, S.L., Péan, C., Berger, S. et al. (2021) IPCC, 2021: climate change 2021: the physical science basis. Contribution of Working Group I to the Sixth Assessment Report of the Intergovernmental Panel on Climate Change.
Matta-El-Amouri, G., Janati-Idrissi, R., Assobhei, O., Petitdemange, H. & Gay, R. (1985) Mechanism of the acetone formation by *Clostridium acetobutylicum* (acetate metabolism; coenzyme A transferase; Clostridium; regulation). *FEMS Microbiology Letters*, 30, 11–16.

17517915, 2024, 2, Downloaded from https://ami-journals.onlinelibrary.wiley.com/doi/10.1111/1751-7915.14414 by Danish Technical Knowledge, Wiley Online Library on [23/02/2024]. See the Terms and Conditions (https://onlinelibrary.wiley.com/terms-and-conditions) on Wiley Online Library for rules of use; OA articles are governed by the applicable Creative Commons License

Mckinney, W. (2010) Data structures for statistical computing in Python. In *Proceedings of the 9th Pyhton in Science Conference*, pp. 56–61.
Monod, J. (1949) The growth of bacterial cultures. *Annual Review of Microbiology*, 3, 371–394.
Munz, C. & Roberts, P.V. (1989) Gas- and liquid-phase mass transfer resistances of organic compounds during mechanical surface aeration. *Water Research*, 23, 589–601.
Nagarajan, H., Sahin, M., Nogales, J., Latif, H., Lovley, D.R., Ebrahim, A. et al. (2013) Characterizing acetogenic metabolism using a genome-scale metabolic reconstruction of *Clostridium ljungdahlii*. *Microbial Cell Factories*, 12, 118.
Nielsen, D.R. & Prather, K.J. (2009) In situ product recovery of *n*-butanol using polymeric resins. *Biotechnology and Bioengineering*, 102, 811–821.
Nikakhtari, H. & Hill, G.A. (2005) Hydrodynamic and oxygen mass transfer in an external loop airlift bioreactor with a packed bed. *Biochemical Engineering Journal*, 27, 138–145.
Noorman, H.J. & Heijnen, J.J. (2017) Biochemical engineering's grand adventure. *Chemical Engineering Science*, 170, 677–693.
Othmer, D.F., Chudgar, M.M. & Levy, S.L. (1952) Binary and ternary Systems of Acetone, methyl ethyl ketone, and water. *Industrial and Engineering Chemistry*, 44, 1872–1881.
Pierce, E., Xie, G., Barabote, R.D., Saunders, E., Han, C.S., Detter, J.C. et al. (2008) The complete genome sequence of *Moorella thermoacetica* (f. *Clostridium thermoaceticum*). *Environmental Microbiology*, 10, 2550–2573.
Pirt, S.J. (1965) The maintenance energy of bacteria in growing cultures. *Proceedings of the Royal Society of London–Series B: Biological Sciences*, 163, 224–231.
Pogrebnyakov, I. & Nielsen, A.T. (2021) Methods and cells for production of volatile compounds.
Pörtner, R. & Faschian, R. (2019) Design and operation of fixed-bed bioreactors for immobilized bacterial culture. In: Mishra, M. (Ed.) *Growing and handling of bacterial cultures*. London: IntechOpen. Available from: https://doi.org/10.5772/intechopen.87944
Price, P.B. & Sowers, T. (2004) Temperature dependence of metabolic rates for microbial growth, maintenance, and survival. *Proceedings of the National Academy of Sciences of The United States of America*, 101, 4631–4636.
Puiman, L., Abrahamson, B., Lans, R.G.J.M., Haringa, C., Noorman, H.J. & Picioreanu, C. (2022) Alleviating mass transfer limitations in industrial external-loop syngas-to-ethanol fermentation. *Chemical Engineering Science*, 259, 117770.
Ragsdale, S.W. & Pierce, E. (2008) Acetogenesis and the Wood-Ljungdahl pathway of CO_2 fixation. *Biochimica et Biophysica Acta*, 1784, 1873–1898.
Redl, S., Diender, M., Jensen, T.Ø., Sousa, D.Z. & Nielsen, A.T. (2017) Exploiting the potential of gas fermentation. *Industrial Crops and Products*, 106, 21–30.
Redl, S., Sukumara, S., Ploeger, T., Wu, L., Ølshøj Jensen, T., Nielsen, A.T. et al. (2017) Thermodynamics and economic feasibility of acetone production from syngas using the thermophilic production host Moorella thermoacetica. *Biotechnology for Biofuels*, 10, 1–17.
Rochón, E., Ferrari, M.D. & Lareo, C. (2017) Integrated ABE fermentation-gas stripping process for enhanced butanol production from sugarcane-sweet sorghum juices. *Biomass and Bioenergy*, 98, 153–160.
Rumble, J.R., Bruno, T.J. & Doa, M.J. (1994) Dependence of boiling point on pressure. In: *CRC handbook of chemistry and physics: a ready-reference*. Boca Raton, FL: CRC Press/Taylor & Francis, p. 497.
Sandberg, T.E., Salazar, M.J., Weng, L.L., Palsson, B.O. & Feist, A.M. (2019) The emergence of adaptive laboratory evolution as an efficient tool for biological discovery and industrial biotechnology. *Metabolic Engineering*, 56, 1–16.
Sander, R. Henry's law constants. (2023) In: Linstrom, P.J. & Mallard, W.G. (Eds.) *NIST chemistry WebBook, NIST standard reference database number 69*. Gaithersburg: National Institute of Standards and Technology.
Scheffen, M., Marchal, D.G., Beneyton, T., Schuller, S.K., Klose, M., Diehl, C. et al. (2021) A new-to-nature carboxylation module to improve natural and synthetic CO2 fixation. *Nature Catalysis*, 4, 105–115.
Schiel-Bengelsdorf, B. & Dürre, P. (2012) Pathway engineering and synthetic biology using acetogens. *FEBS Letters*, 586, 2191–2198.
Servais, P., Billen, G., Rego, J.V. & Vives, J. (1985) Rate of bacterial mortality in aquatic environments. *Applied and Environmental Microbiology*, 49, 1448–1454.
Shuler, M.L. & Kargi, F. (2002) 7.3. Stoichiometric Calcluations. In: *Bioprocess engineering: basic concepts*. Upper Saddle River: Prentice Hall, pp. 209–216.
Steger, F., Ergal, İ., Daubek, A., Loibl, N., Rachbauer, L., Fuchs, W. et al. (2022) Trickle-bed bioreactors for Acetogenic H_2/CO_2 conversion. *Frontiers in Energy Research*, 10, 307.
Tijhuis, L., Van Loosdrecht, M.C.M. & Heijnen, J.J. (1993) A thermodynamically based correlation for maintenance gibbs energy requirements in aerobic and anaerobic chemotrophic growth. *Biotechnology and Bioengineering*, 42, 509–519.
Tschaplinski, T.J. & Simpson, S.D. (2019) Development of a Sustainable Green Chemistry Platform for Production of Acetone and Downstream Drop-in Fuel and Commodity Products Directly From Biomass Syngas Via a Novel Energy Conserving Route in Engineered Acetogenic Bacteria.
van Baten, J.M. & Krishna, R. (2004) Scale effects on the hydrodynamics of bubble columns operating in the heterogeneous flow regime. *Chemical Engineering Research and Design*, 82, 1043–1053.
Vees, C.A., Neuendorf, C.S. & Pflügl, S. (2020) Towards continuous industrial bioprocessing with solventogenic and acetogenic clostridia: challenges, progress and perspectives. *Journal of Industrial Microbiology and Biotechnology*, 47, 753–787.
Verhoef, S., Wierckx, N., Westerhof, R.G.M., De Winde, J.H. & Ruijssenaars, H.J. (2009) Bioproduction of p-hydroxystyrene from glucose by the solvent-tolerant bacterium *Pseudomonas putida* S12 in a two-phase water-decanol fermentation. *Applied and Environmental Microbiology*, 75, 931–936.
Virtanen, P., Gommers, R., Oliphant, T.E., Haberland, M., Reddy, T., Cournapeau, D. et al. (2020) SciPy 1.0: fundamental algorithms for scientific computing in Python. *Nature Methods*, 17, 261–272.
Wen, H., Chen, H., Cai, D., Gong, P., Zhang, T., Wu, Z. et al. (2018) Integrated in situ gas stripping-salting-out process for high-titer acetone-butanol-ethanol production from sweet sorghum bagasse. *Biotechnology for Biofuels*, 11, 134.
Whitman, W.G. (1962) The two film theory of gas absorption. *International Journal of Heat and Mass Transfer*, 5, 429–433.
Wieringa, K.T. (1936) Over het verdwijnen van waterstof en koolzuur onder anaerobe voorwaarden. *Antonie Van Leeuwenhoek*, 3, 263–273.
Wood, H.G. & Harris, D.L. (1951) A study of carbon dioxide fixation by mass determination of the types of C^{13}-acetate. *The Journal of Biological Chemistry*, 194, 905–931.
Xue, C., Liu, F., Xu, M., Zhao, J., Chen, L., Ren, J. et al. (2016) A novel *in situ* gas stripping-pervaporation process integrated with acetone-butanol-ethanol fermentation for hyper n-butanol production. *Biotechnology and Bioengineering*, 113, 120–129.
Zeldes, B.M., Keller, M.W., Loder, A.J., Straub, C.T., Adams, M.W.W. & Kelly, R.M. (2015) Extremely thermophilic microorganisms as metabolic engineering platforms for production of fuels and industrial chemicals. *Frontiers in Microbiology*, 6, 1209.
Zhang, Z., Li, Y., Zhang, J., Peng, N., Liang, Y. & Zhao, S. (2020) High-titer lactic acid production by *Pediococcus acidilactici*

17517915, 2024, 2, Downloaded from https://ami-journals.onlinelibrary.wiley.com/doi/10.1111/1751-7915.14414 by Danish Technical Knowledge, Wiley Online Library on [23/02/2024]. See the Terms and Conditions (https://onlinelibrary.wiley.com/terms-and-conditions) on Wiley Online Library for rules of use; OA articles are governed by the applicable Creative Commons License

PA204 from corn stover through fed-batch simultaneous saccharification and fermentation. *Microorganisms*, 8, 1–9.

Zheng, T., Zhang, M., Wu, L., Guo, S., Liu, X., Zhao, J. et al. (2022) Upcycling CO_2 into energy-rich long-chain compounds via electrochemical and metabolic engineering. *Nature Catalysis*, 5, 388–396.

SUPPORTING INFORMATION

Additional supporting information can be found online in the Supporting Information section at the end of this article.

How to cite this article: Gorter de Vries, P.J., Mol, V., Sonnenschein, N., Jensen, T.Ø. & Nielsen, A.T. (2024) Probing efficient microbial CO_2 utilisation through metabolic and process modelling. *Microbial Biotechnology*, 17, e14414. Available from: https://doi.org/10.1111/1751-7915.14414

17517915, 2024, 2, Downloaded from https://ami-journals.onlinelibrary.wiley.com/doi/10.1111/1751-7915.14414 by Danish Technical Knowledge, Wiley Online Library on [23/02/2024]. See the Terms and Conditions (https://onlinelibrary.wiley.com/terms-and-conditions) on Wiley Online Library for rules of use; OA articles are governed by the applicable Creative Commons License